energy&fuels

pubs.acs.org/EF
Article

Biobased Vanillin Production by Oxidative Depolymerization of Kraft Lignin on a Nitrogen- and Phosphorus-Functionalized Activated Carbon Catalyst

Miguel García-Rollán, Maria N. Rivas-Márquez, Salvador Bertran-Llorens, Peter J. Deuss, Ramiro Ruiz-Rosas, Juana M. Rosas,* José Rodríguez-Mirasol, and Tomás Cordero

Cite This: *Energy Fuels* 2024, 38, 7018−7032

ABSTRACT: The sustainable production of vanillin from the oxidative depolymerization of lignin was evaluated. Vanillin was produced from Kraft lignin using heterogeneous catalysts based on activated carbons prepared by chemical activation of sodium lignosulfonate with H_3PO_4. The novel redox catalytic system, obtained by HNO_3 treatment, allows the heterogenization of nitrobenzene structures on the activated carbon, reaching vanillin yield 30% higher than that obtained without a heterogeneous catalyst (about 3.1 wt %). A copper catalyst (5 wt %) was also prepared for comparison purposes. The highest vanillin yield was obtained at 200 °C and 10 bar for the nitrobenzene-like catalyst, reaching full extraction from the selected technical lignin. The catalyst was successfully reused without any regeneration treatment, evidencing no signs of deactivation. The possibility of transferring oxygen from oxidized P groups to reduced N groups in a redox cycle seems to be responsible for this sustained catalytic activity. To promote zero waste production, the obtained residual lignin was also used to prepare an activated carbon with outstanding properties, $A_{BET} \sim 1000$ m^2/g.

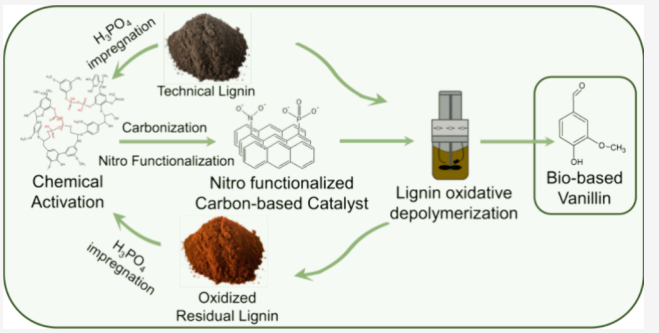

1. INTRODUCTION

Lignin is a three-dimensional, heterogeneous macromolecule that holds together the structure of the cell walls. It is, along with cellulose and hemicellulose, one of the three main constituents of lignocellulosic biomass. It is formed by the oxidative polymerization of three types of hydroxycinnamyl alcohols, known as monolignols.[1,2] These three main units are *p*-hydroxyphenyl (H), guaiacyl (G), and syringyl (S), which are linked through different types of carbon−carbon or ether bonds, such as *β*-O-4, *α*-O-4, 5-O-4, *β*-5, *β*-1, *β*-*β*, or 5-5,[2] of which *β*-O-4 is dominant, accounting for 40−60% of the total of the linkage structures of lignin.[3,4] The relative abundance of monolignols and the nature and amount of ether bonds vary from plant to plant, being known that softwoods have a majority of G-units (approximately 90%), while hardwoods have a similar amount of G- and S-units,[5] by the extraction method used for lignin isolation. Thus, if the extraction conditions are harsher, the technical lignin obtained will have a high concentration of C−C bonds to the detriment of *β*-O-4 ones.

Lignin may have a huge valorization potential due to its aromatic structure and being unique in nature; however, it is currently mainly burned in the pulp and paper industry to produce energy for mill self-sufficiency. As a more environmentally friendly alternative, the production of chemicals with high added value from lignin has been proposed in the literature. Many processes are envisaged for this purpose, such as the pyrolysis process for bio-oil production,[6] syngas from lignin gasification,[7] BTX from lignin hydrodeoxygenation (HDO),[8] cycloalkane production via hydrogenation,[9] or the obtention of monoaromatic aldehydes from oxidative depolymerization of lignin,[10] where vanillin stands out as the most profitable compound.

Vanillin is a high-value aromatic aldehyde, which is used as a flavor and fragrance ingredient in the food industry and as a platform molecule in pharmacology. Less than 1% of the world's vanillin production is extracted from vanilla pods. More than 80% of the vanillin world production comes from the Riedel process.[11] The remaining production (around 15%) comes from oxidative depolymerization of residual lignins.[12] This last process yields reasonably large amounts (the vanillin yield does not exceed 5% due to the condensed structure of

Received: January 8, 2024
Revised: March 25, 2024
Accepted: March 25, 2024
Published: April 4, 2024

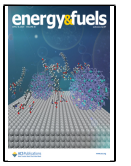

https://doi.org/10.1021/acs.energyfuels.4c00108
Energy Fuels 2024, 38, 7018−7032

industrial technical lignins) of single monomeric aldehydes from technical lignins. Specifically, vanillin is the main product of the oxidation of softwood lignins, richer in G-units; meanwhile, hardwood lignins yield a mixture of vanillin and syringaldehyde due to their higher presence of S-units. In addition, some new uses include stimulating the production of biobased vanillin, such as a substitute of petro-based building blocks or in the synthesis of polycarbonates[13] or polyesters.[14]

To maximize the yield of vanillin during the oxidative depolymerization of lignin, several considerations should be made. First, the origin of the technical lignin and the extraction method used for its isolation strongly affect the structure of lignin, i.e., the monolignols and the β-O-4 structural content, respectively, being possible to obtain Kraft-type lignins, lignosulfonates, or even organosolv lignins and, therefore, the vanillin yield. Since vanillin comes from the oxidation of the guaiacyl groups present in the lignin structure, the selectivity of the process will be improved if lignins from softwoods are used.[15] Second, the yield is affected by the pH used in oxidative depolymerization. Although there have been some recent studies using acidic or even ionic liquid media,[16] alkaline conditions are the most widely studied in the literature[17] and are the ones currently exploited at the industrial level.[18] For instance, the oxidation of Kraft lignin in an alkaline medium to produce vanillin must be carried out at pH above 12 to avoid the protonation of the anion formed as a reaction intermediate species or the overoxidation of vanillin into other chemicals.[19] Finally, the oxidation agent also plays a critical role in the vanillin yield. The oxidants used are oxygen, CuO,[20] and nitrobenzene, with other oxidants being H_2O_2,[21] peroxodicarbonate,[22] and oxides of transition metal, which are less explored. Among all, oxygen is the most used oxidizing agent due to its low cost and high availability; however, it has certain drawbacks, such as the fact that it can produce overoxidation of technical lignin, its low solubility in the reaction medium, and the need of work at relatively high temperature.[15] Regarding oxidation of lignin with nitrobenzene, it is a long-known process[23,24]; however, nitrobenzene is very toxic, and the reaction product generated after its consumption, aniline, is even more so. In addition to its dangerousness, its higher cost than molecular oxygen is the main reason for its industrial use being discarded, in spite of it being a much more selective reagent than its counterparts.[25]

With regard to the catalyst used in this reaction, the studies are focused on increasing selectivity toward vanillin, because phenolate anions, which appeared in the reaction media as intermediate species, have one of the most oxidable functional groups. The stability of certain phenolic derivatives, produced by this route, has been studied to propose the corresponding oxidation mechanism.[26] For this purpose, the redox potential of the catalyst should be low but high enough to oxidize the phenolate anion. Thus, species such as Cu salts, which have a moderate redox potential, are good candidates for the biobased vanillin production from lignin.[27] Homogeneous catalysts such as transition metal salts or oxides, i.e., $CuSO_4$, $FeCl_3$, CuO, and Fe_2O_3,[28] different polyoxometalates,[29,30] or even other redox catalysts[31] are preferred in terms of productivity. Even though homogeneous catalysts improve the mass transfer rate, the difficulties for their separation and recovery and the high purity requirements of the product hinder their use. Heterogeneous catalysts, widely used in lignin depolymerization reactions,[32] may circumvent these drawbacks, yet they may also face diffusional limitations of the lignin fragments produced during the alkaline homolysis. Some of the heterogeneous catalysts used in this reaction are those based on CeO_2,[33] γ-Al_2O_3,[34] MOF,[35,36] hydrotalcite,[37] and activated carbons[38] with different active phases such as Pd, Co, Fe_2O_3, and CuO.

On the other hand, lignin can be also valorized through the preparation of carbon materials with high industrial interest.[39] In this regard, researchers in this field have made a great effort carrying out studies on the production of activated carbons, carbon fibers, and other carbon materials from different technical lignins.[40] Particularly, the activated carbons (ACs) are porous carbon materials with a highly developed specific surface area, which can be used in different applications such as adsorption,[41] energy storage,[42] or catalysis as catalytic support[43] or a catalyst by itself.[44] The advantages of using AC as a catalyst are (i) easily modifiable surface chemistry, (ii) tunable porosity with macro-, meso-, and/or micropores, which allow optimum diffusion of the reagents to the pores and adequate distribution of the active phase,[41] (iii) strong chemical resistance, and (iv) relatively low production costs. Despite all the advantages of using carbon materials as a catalyst or catalytic support for chemical reactions, there are very few studies in the literature using carbon- or graphene-based catalysts for the oxidative depolymerization reaction of lignins.[45−47] This fact may be associated with the probable oxidation of the activated carbon under the conditions used for biobased vanillin production. However, ACs produced by chemical activation of lignocellulosic waste with H_3PO_4 present phosphorus surface groups of high thermal and chemical stability that lead to the AC high resistance to oxidation.[48] Previously, we have demonstrated that nitro-functionalities can be inserted, with high dispersion, into the surface of H_3PO_4 activated carbons through a nitric acid treatment,[49] making it possible to obtain a heterogeneous catalyst with nitro groups as active sites. In this way, the disadvantages of having to add nitrobenzene to this reaction are circumvented, making the process more environmentally friendly. This fact could enable its inclusion within the pulp and paper industry or in a lignocellulosic biorefinery, boosting the circular bioeconomy goals. Furthermore, the use of lignin for the preparation of the catalytic support could also enhance the process sustainability and make it more feasible to reach a zero waste biorefinery operation.

Therefore, this work proposes the use of an activated carbon obtained through the chemical activation of sodium lignosulfonate with phosphoric acid, loaded with copper or functionalized with nitro groups, as a catalyst for the oxidative depolymerization reaction of lignin to obtain biobased vanillin.

2. MATERIALS AND METHODS

2.1. Materials. Indulin-AT, a pine (softwood) wood Kraft lignin, was kindly provided by the green chemical reaction engineering group of ENTEG (Engineering and Technology institute Groningen) from the Groningen University, The Netherlands, and was produced by the Westvaco Chemical Division, Charleston Heights. This commercial lignin is recovered and purified from black liquor of Kraft pulping of pine wood (97% of lignin content on a dry basis). HANSA-201 (sodium lignosulfonate) was supplied by Sappi Biotech GmbH, Stockstadt, Germany, and was isolated from *Eucalyptus* (hardwood). Other lab-supply grade reagents, such as H_3PO_4 (85%, Fluka), HCl (≥37%, Fluka), NaOH (98%, PanReac AppliChem), ethyl acetate anhydro (99.8%, Sigma-Aldrich), acetone (HPLC grade, PanReac AppliChem), guaiacol (≥98%, Sigma-Aldrich), 4-hydroxybenzaldehyde (98%, Sigma-Aldrich), vanillic acid (97%, Sigma-Aldrich), and

https://doi.org/10.1021/acs.energyfuels.4c00108
Energy Fuels 2024, 38, 7018−7032

vanillin (99%, Sigma-Aldrich), were used. N_2 and O_2 (99.995% purity) were supplied by Air Liquide.

2.2. Catalyst Preparation. Sodium lignosulfonate was selected as a carbonaceous precursor for the synthesis of H_3PO_4 chemically activated carbons (AC). Sodium lignosulfonate was mixed with H_3PO_4 at room temperature and kept at 60 °C for 24 h. The weight impregnation ratio (H_3PO_4/carbon precursor) was set in 3; thus, in each batch, 5 g of sodium lignosulfonate was impregnated with 17.7 g of an 85% H_3PO_4 solution. The impregnated sample was then activated under a N_2 continuous flow (150 Ncm^3/min) in a conventional tubular furnace (Hobersal) at 500 °C for 2 h with a heating ramp of 10 °C/min. The activated sample was then washed with deionized water at 60 °C until constant pH in the eluate to remove the excess of phosphorus. The resulting material was dried and sieved between 100 and 400 μm. The solid yield of the whole process after subtracting the humidity and ash content was 35%.

To obtain an activated carbon functionalized with nitro groups, the AC was submitted to a treatment with nitric acid as detailed elsewhere.[49] Briefly, 1 g of AC was introduced in a round-bottom flask with 50 mL of a 5 M HNO_3 solution at 80 °C for 3 h. After the acid treatment, the sample was washed several times with deionized water to remove the excess of nitric acid.

For the sake of comparison, the Cu metallic phase, typically used as a catalyst species in the biobased vanillin production, was incorporated to the activated carbon by the incipient wetness impregnation method using a solution of $Cu(NO_3)_2{\cdot}3H_2O$. The impregnated material with enough copper salt to reach 5% wt in the final catalyst was dried at 110 °C for 12 h, and then the sample was heated at 450 °C for 4 h under a N_2 continuous flow (150 Ncm^3/min), in a tubular furnace, to decompose the copper salt and to obtain the active phase. The nitro-functionalized activated carbon sample was named ACN, while ACCu was used to refer to the activated carbon loaded with Cu.

2.3. Oxidation Experiments and Product Analysis. Oxidation experiments with O_2 in an alkaline medium were performed in a Demede Engineering and Research stirred batch reactor with a capacity of 100 mL. The setup is equipped with a magnetic stirrer, temperature, pressure control system, and sample collection port. In a typical essay, 2 g of Indulin-AT lignin is dissolved in 50 mL of a 40 g/L solution of NaOH (pH = 14) and introduced in a stainless-steel flask. If the reaction is carried out with a heterogeneous catalyst, once lignin has been dissolved in the 40 g/L NaOH solution, 30 mg of catalyst is added to the solution and then the stainless-steel flask is placed into the reaction system. The charged reactor was purged with pure O_2 three times, and the system was pressurized with O_2 to a pressure of 5 bar. The reaction system was then heated, at a heating rate of 15 °C/min, at temperatures between 125 and 225 °C, reaching a maximum pressure corresponding to the autogenous pressure of the system, i.e., the vapor pressure of a 40 g/L NaOH solution at the reaction temperature. During the reaction, a collection system was used that allowed the extraction of 0.5 mL of the liquid phase without any disturbance of the pressure inside of the reaction system to analyze the liquid products at different reaction times. In all of the experiments, the temperature and pressure were recorded to study the performance of the gas phase and check that the extraction of sample aliquots did not alter the state of the reaction. With the aim of ensuring, all experiments were carried out in triplicate.

The procedure for the analysis of the different species after the reaction is summarized in Scheme S1. Upon removal of the stainless-steel flask from the reaction system, the sample includes a solid, the carbon-based catalyst, and a liquid phase consisting of the reaction products and unreacted lignin in solution. First, the catalyst was removed by a filtering process and then a volume of a concentrated HCl solution was added until pH = 2 was reached to precipitate the unreacted lignin. The precipitated unreacted lignin was removed by another filtration process. To separate the aqueous phase from the organic phase, which remains in the solid-free liquid sample, an extraction process was carried out, washing several times the solid-free liquid sample with ethyl acetate until a transparent color in the aqueous phase was reached. Ethyl acetate was evaporated under vacuum to obtain a concentrated liquid phase, which was diluted 1:40 in acetone, and then a 1.5 mL aliquot of the solution was transferred to a glass vial where 7.5 μL of an external standard, dodecane, was added. This new solution was analyzed in a gas chromatograph coupled to a mass spectrometer Agilent 7000 D GC/MS Triple Quad (GC-MS), equipped with a 60 m DB-624 column, using a FID and with the mass spectrometer working on SIM mode following the signals of the main reaction components. The chromatographic method started at 60 °C, with a final temperature of 240 °C, a heating rate of 8 °C/min, and a holding time of 20 min. To determine the concentration of the main products of the process, prior to analyzing the liquids of each reaction, calibration curves of vanillin, guaiacol, and acetovanillone (the main products of the reaction, as shown in Figure S1) were made using concentrations in the range of 50 and 3.125 ppm.

The postreaction gases were analyzed by GC using a TCD and carbon-plot column. Only oxygen was observed since the possible CO_2 formed by mineralization of lignin is able to react with sodium hydroxide to form carbonates (confirmed by the pH drop at the end of reaction, from 13.6 to 13.2−13.0), therefore avoiding its release in the gas phase.

In addition, unreacted lignin was dried at 60 °C overnight and then activated under the same operating conditions as the AC from sodium lignosulfonate.

Thus, the conversion and the different oxidation product selectivity and yield were calculated as follows:

$$\text{conversion}(\%) = \frac{\text{initial lignin wt} - \text{residual lignin wt}}{\text{initial lignin wt}} \times 100$$

$$\text{selectivity}(\%) = \frac{\text{product wt}}{\sum \text{product wt}} \times 100$$

$$\text{product yield}(\%) = \frac{\text{product wt}}{\text{initial lignin wt}} \times 100$$

The solid residue obtained at the end of the reaction, after neutralization with HCl, was composed of a mixture of oxidized lignin and NaCl. To determine the amount of oxidized lignin, the solid residue was filtered and dried at 100 °C overnight. A sample of 100 mg of the dried solid was calcined at 750 °C to constant weight, considering that the organic matter removed during the calcination process was the so-called "residual lignin". This procedure was replicated three times.

For the catalyst reusability test, the catalyst was filtered and separated from the product stream, dried in a vacuum oven overnight, and then tested, without any regeneration process, under the same operating conditions as the fresh catalyst.

2.4. Characterization of the Samples. The chemical composition of the technical lignins was evaluated by the ultimate analysis of the samples in CNHS EA3000 equipment. The composition of technical lignins was also analyzed by proximate analysis to know the quantity of volatile matter (ASTM E-872), ash content (ASTM E-1755), and fixed carbon determined, by difference, of the samples. The inorganic composition of the technical lignins was also analyzed by X-ray fluorescence (XRF) in THERMO ARL PERFORM'X equipment.

The porosity of the activated carbons was studied by N_2 adsorption−desorption at −196 °C and CO_2 adsorption at 0 °C using Micromeritics ASAP2020 equipment. They were degassed for at least 8 h at 150 °C. The specific surface area (A_{BET}) was obtained using the BET equation following the criteria proposed by Rouquerol for the selection of the fitting region from N_2 adsorption isotherms. The micropore volume (V_s) and external surface area (A_s) were calculated using the α-s method, and the mesopore volume (V_{mes}) was estimated as the difference between the adsorbed volume at a relative pressure of 0.98 and the micropore volume (V_s). The narrow micropore volume (V_{DR}) and surface area (A_{DR}) were determined, applying the Dubinin−Radushkevich method in the CO_2 adsorption isotherms. Finally, the pore size distribution was obtained from the N_2

https://doi.org/10.1021/acs.energyfuels.4c00108
Energy Fuels 2024, 38, 7018−7032

and CO_2 adsorption isotherms by using the 2D-NLDFT heterogeneous surface model.[50]

The functional groups of the samples were semiquantified using a Fourier transform infrared (FTIR) spectrometer (Bruker Optics Vertex 70) in the attenuated total reflectance (ATR). The spectra were acquired at a resolution of 4 cm^{-1}, and 64 scans were taken in the 600−4000 cm^{-1} range. To analyze the oxidation state of surface species of the fresh technical lignins, the activated carbons, and the residual lignin after reaction, X-ray photoelectron spectroscopy (XPS) analyses were carried out by using PHI 5700 equipment with a monochromatic Al Kα radiation source (1486.6 eV). The maximum of the C 1s peak was set to the XPS photoemission energy of the C−C and C═C bonds (284.5 eV) as the reference.

Carbon materials present different oxygenated groups, which decompose as CO and/or CO_2 at different temperature ranges, allowing the determination of their nature and quantity by temperature-programmed desorption (TPD). TPD experiments were carried out with 80 mg of a dry sample loaded in a quartz reactor. The reactor was heated from room temperature to 900 °C at 10 °C/min in a N_2 flow of 150 N mL/min. The quantities of CO and CO_2 evolved during the heating process were monitored in a nondispersive infrared (NDIR) gas analyzer, Siemens ULTRAMAT 23. To assess the total acidity and the acid strength of the carbon-based catalysts, temperature-programmed desorption of ammonia (TPD-NH_3) was carried out. TPD-NH_3 was carried out in two different steps. Initially, as a blank experiment, 50 mg of fresh catalyst was submitted to thermally programmed desorption in the absence of ammonia, heating it from room temperature to 500 °C with a heating rate of 10 °C/min. Subsequently, in the TPD-NH_3 experiment, another batch of 50 mg of fresh catalyst was saturated with NH_3 for 15 min at 100 °C, and then a flow of He removed the weakly adsorbed NH_3 at the adsorption temperature for enough time to not detect NH_3 at the reactor outlet. NH_3 desorption was carried out by increasing the temperature from 100 to 500 °C at 10 °C/min using a thermal conductivity detector (TCD) as a detector. Finally, the TPD-NH_3 profile will be the result of subtracting the signal of the blank experiment from TPD-NH_3. To evaluate the morphology of the support and catalysts, transmission electron microscopy (TEM) images were taken using an FEI Talos F200X microscope at 200 kV.

Fresh and unreacted lignin was analyzed by 2D-HSQC-NMR. The spectra were collected from a 600 MHz Bruker Biospin (Rheinstetten, Germany, BASIC PROBHD) instrument with the following parameters: spectra use 1024 data points from 11 to 2.35 ppm in ^1H (acquisition time, 131 ms) and 160 to 35 ppm in ^{13}C with 256 increments (acquisition time, 6 ms) of 8 scans with 1.5 s of internal delay; the d24 delay was set to 86 ms. The signal of dimethyl sulfoxide (DMSO) solvent was used as an internal reference (δC 39.5, δH 2.49 ppm).

3. RESULTS AND DISCUSSION

3.1. Technical Lignin Characterization. Considering the above stated in Section 1, organosolv lignin would be the most appropriate lignin for vanillin production based on its structural properties, i.e., higher amount of β-O-4 bonds. However, this type of material is not widespread in the market and is not broadly considered as waste product,[51] so in this study, it has been decided to select some type of industrial lignin as the main feedstock for its oxidative depolymerization process. Thus, Table 1 shows the most relevant properties of Kraft lignin and sodium lignosulfonate used in this work. The proximate analysis reveals that the ash content in sodium lignosulfonate is higher than in Kraft lignin or even in other technical lignins reported in the literature.[52−54] The presence of large amounts of ashes in the reaction media could cause detrimental effects over the process, i.e., fouling of the reaction system or poisoning of the catalyst and reaction products. In this sense, the use as feedstock of Kraft lignin for the depolymerization reaction could be more appropriate. This premise is also reinforced when the low volatile matter content of sodium lignosulfonate is considered, given that volatile matter is directly related to the amount of lignin fragments that are most susceptible to being transformed to oxidative depolymerization products.

Table 1. Analytical Characteristics of the Technical Lignins

	Kraft lignin	sodium lignosulfonate
proximate analysis (%d.b.)[a]		
volatile matter	55.6	52.3
ash content	2.7	16.9
fixed carbon	41.7	30.8
ultimate analysis (%dry ash free)		
C	62.3	39.9
H	6.0	5.3
N	0.8	0.2
S	1.2	4.6
O[b]	29.8	50.0
XPS analysis (% wt)		
C	71.4	50.6
N	0.6	0.8
O	26.5	31.9
Na	0.4	9.8
S	1.2	6.9
XRF analysis (% wt)		
S	0.7	3.3
Na	0.3	6.2
others	0.2	0.3

[a]Dry basis. [b]By difference.

Figure 1 represents the corresponding FTIR spectra of Kraft lignin and sodium lignosulfonate. The FTIR spectra confirm the presence of sulfone groups (655 cm^{-1}) in sodium lignosulfonate[55] and thiol-thioesters (812 cm^{-1}) in Kraft lignin.[56] Such groups are also noticeable in the S 2p XPS spectra (Figure S2) of both technical lignins. In addition, sodium lignosulfonate shows a poorly defined peak centered about 1212 cm^{-1} that corresponds to condensed G-units.[57,58] This peak is more intense in the case of Kraft lignin. As mentioned in Section 1, typically, the content of monolignol units as well as the presence of aryl ether or carbon−carbon bonds varies in the technical lignins depending on the lignocellulosic precursor and lignin isolation method, respectively. Usually, the harsher the extraction conditions, the less aryl ether linkages are maintained, while more C−C bonds are formed, and thus, the condensation degree of the lignin structure is larger. The Kraft method uses more severe conditions during extraction (7−10 atm, 180 °C, and 0.5−2 h) than the sulfite process (8−12 h, at 110−145 °C, and at a pressure of 6−7 atm), explaining the higher intensity of the 1212 cm^{-1} peak found in Kraft lignin, due to a higher presence of condensation reactions during the isolation process.

Figure 2 represents the 2D HSQC NMR spectra of the two technical lignins studied in this work. The main signals of the aliphatic regions are identified corresponding to the S-, G-, or H-units, as well as their oxidized and condensed modifications according to a previous report.[59] The S/G ratio is much lower than 1 in the case of Kraft lignin (Table 2). The main linkages present in lignin, i.e., β-O-4, $\beta-\beta$ and β-5, are represented by blue-, green-, and violet-colored signals in the aliphatic region of the NMR. The amount of β-O-4 linkages seems to be higher in Kraft lignin than its counterpart. Moreover, a higher and

https://doi.org/10.1021/acs.energyfuels.4c00108
Energy Fuels 2024, 38, 7018−7032

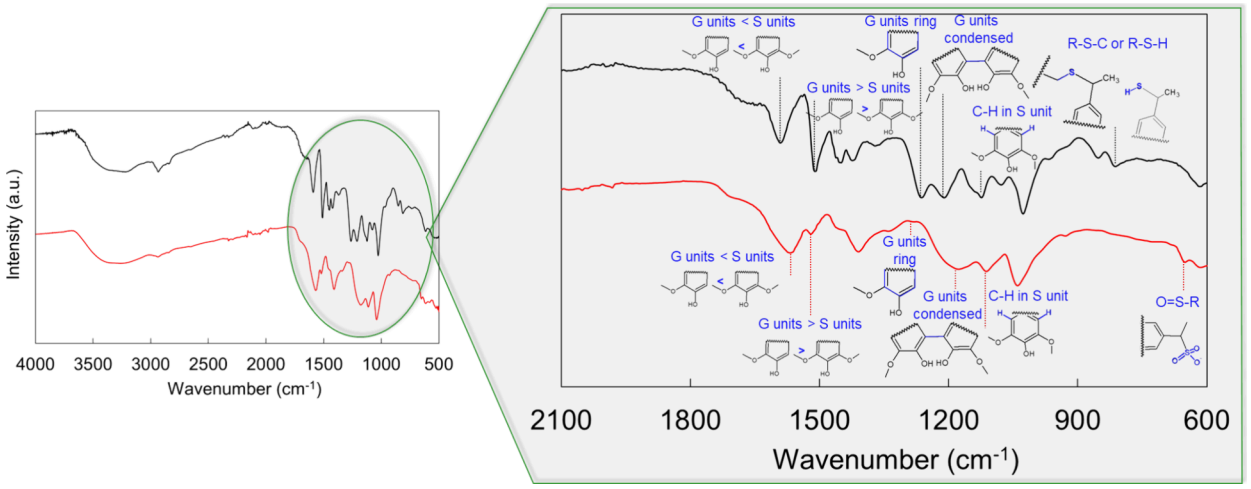

Figure 1. FTIR spectra of Kraft lignin (black line) and sodium lignosulfonate (red line).

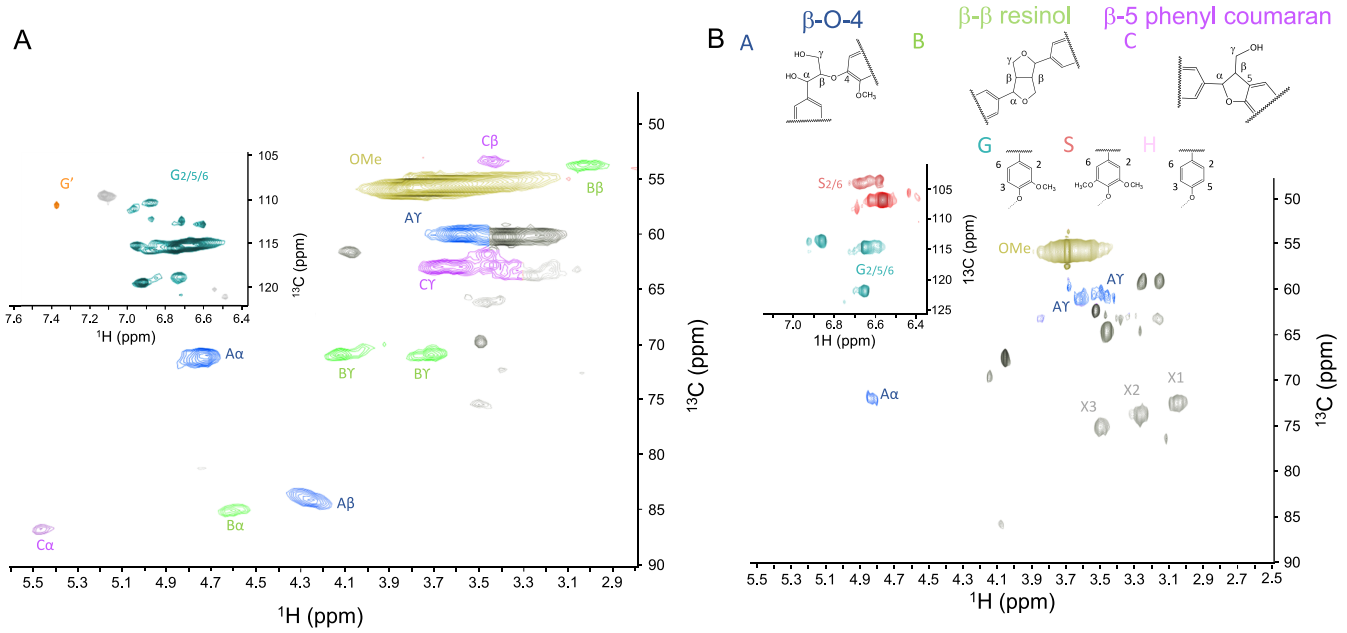

Figure 2. 2D HSQC NMR spectra of Kraft lignin (A) and sodium lignosulfonate (for proper visualization of the NMR spectra, aliphatic regions are 2× intensified than aromatic regions) (B).

Table 2. Main Aromatic Units and Linkages in Technical Lignins Obtained by Semiquantification of the 2D HSQC NMR Spectra Shown in Figure 2

technical lignin	S[a]	G[b]	H[c]	β-O-4[d]	β-β	β-5	S/G
Kraft lignin	0.0	95.9	4.1	10.6	3.4	2.7	0.0
sodium lignosulfonate	60.4	38.5	1.1	7.6	0.0	1.6	1.6

[a] $S = \frac{S_{2/6} + S'_{2/6}}{2} \cdot \frac{1}{\text{total aromatics}} \cdot 100$ [b] $G = \frac{G_2 + G_5 + G_6 - H_{2/6} - G' \cdot 2}{3} \cdot \frac{1}{\text{total aromatics}} \cdot 100$ [c] $H = \frac{H_{2/6}}{2} \cdot \frac{1}{\text{total aromatics}} \cdot 100$ [d]Linkages are expressed per 100 aromatic units.

more selective biobased vanillin yield is expected from depolymerization of Kraft lignin owing to a larger amount of G-units (Table 2).

For these reasons, Kraft lignin has been selected as feedstock in the oxidative depolymerization to yield biobased vanillin; meanwhile, sodium lignosulfonate, less rich in the *β*-O-4 bond, will be valorized through the production of an activated carbon-based catalyst.

3.2. Characterization of Catalysts. Figure 3 shows the N_2 adsorption−desorption isotherm at −196 °C and the pore size distribution of the catalysts and the catalyst support. All carbon materials have a type IV isotherm characteristic of mesoporous materials. Moreover, the hysteresis cycle seems to be a combination of the H1 and H3 types.[60] The high N_2 uptake at low relative pressures in these materials evidences the large presence of micropores. The shape of the adsorption−desorption isotherm at medium−large relative pressures suggests the presence of well-developed mesoporosity and macroporosity, which can be useful to minimize mass transfer limitations that are usually found for oxidative depolymerization of lignin.[61] The main textural parameters are given in Table 3. All of the samples present apparent surface areas

https://doi.org/10.1021/acs.energyfuels.4c00108
Energy Fuels 2024, 38, 7018−7032

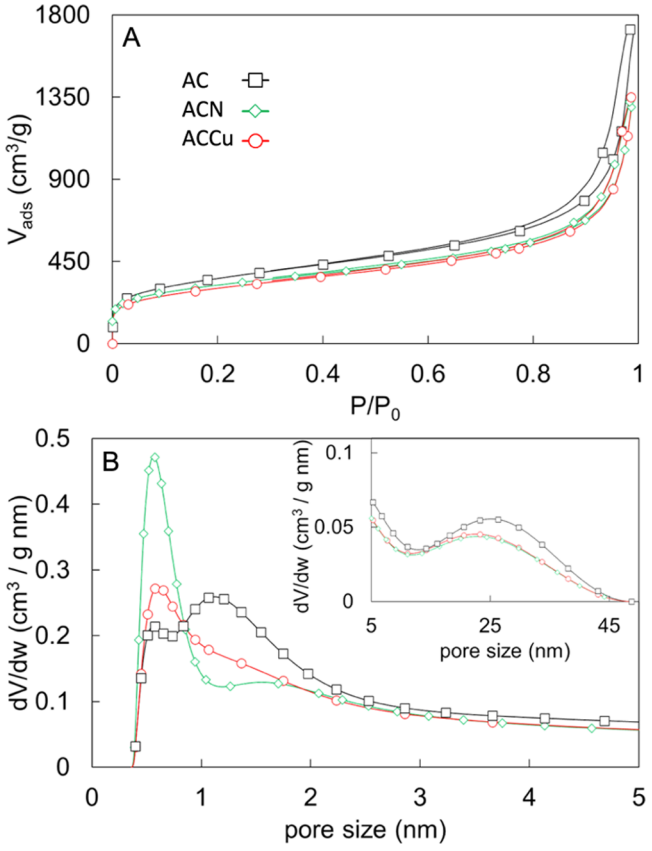

Figure 3. N_2 adsorption−desorption isotherms obtained at −196 °C (A) and pore size distribution calculated from the N_2 adsorption−desorption isotherm and CO_2 adsorption isotherm at −196 and 0 °C, respectively (B), of AC, ACN, and ACCu.

Table 3. Summary of the Textural Parameters Obtained from the N_2 Adsorption−Desorption Isotherm and CO_2 Adsorption Isotherm Obtained at −196 and 0 °C, Respectively, CO and CO_2 Evolved Amounts from TPD, and Mass Surface Concentration Derived from XPS Analyses of the Carbon Materials

sample	AC	ACN	ACCu
N_2 ads−des isotherm			
A_{BET} (m^2/g)	1290	1150	1090
V_{meso} (cm^3/g)	1.86	1.51	1.46
V_s (cm^3/g)	0.37	0.33	0.30
$V_{0.995}$ (cm^3/g)	2.68	2.10	2.10
CO_2 ads isotherms			
V_{DR} (cm^3/g)	0.19	0.22	0.16
TPD (μmol/g)			
CO_2	172	1918	1070
CO	1586	4416	3487
O	1930	8251	5627
XPS (wt %)			
C	89.6	75.8	87.5
O	8.4	20.2	9.1
P	2.0	1.2	1.9
N	–	2.7	–
Cu	–	–	1.5

larger than 1000 m^2/g and pore volumes higher than 2 cm^3/g. The wide pore structure of the samples is confirmed by the higher contribution of mesopore volumes (V_{meso}), being 5 times higher than that of the micropores (V_s). This wide pore texture minimizes the presence of internal mass transport limitations, which are typically found in this reaction. The higher value of the micropore volume measured by N_2 adsorption, V_S, compared to micropore volume obtained by CO_2 adsorption, V_{DR}, suggests the presence of micropores with an average size larger than 0.7 nm.[62] In addition, as can be seen in Figure 3B, all materials have a bimodal distribution with a maximum centered around 1.2 nm and another at 26 nm. It is worth highlighting the notable reduction in mesoporosity, i.e., almost 20%, in the case of both catalysts ACCu and ACN, attributable to the pore blockage and partial gasification of the carbon particles, respectively,[49] as well as an increase in the narrow microporosity (see Figure 3B), which in the latter case, may be explained through the anchoring of the nitro groups on the carbon surface, hindering the access to micropores.

Previous studies reported that the moderate acidity of activated carbons produced by chemical activation with phosphoric acid, as exhibited by the catalysts studied in this research (Figure S4A), is a consequence of the presence of polyphosphates with C−O−P bonds tightly bound to the carbon network that exhibit high thermal and chemical stability.[63] Thus, surface characterization with techniques such as XPS to determine both the content and oxidation state of phosphorus is essential in this type of material.[64] Figure 4A represents the XPS spectra of the P 2p region of the carbon materials. The catalyst P 2p spectrum can be deconvoluted in two peaks centered at binding energies of 133.4 and 134 eV characteristic of tetracoordinated phosphorus (PO_4) in phosphates and/or polyphosphates[65] and the photoelectronic excitation of phosphorus when it is bonded to carbon through an oxygen, forming the C−O−P bond,[66] respectively. The presence of C_3PO surface groups (observed at 131 and 132 eV) can be ruled out in these catalysts.[67] On the other hand, although the amounts of surface P on the AC and ACCu samples are very similar, 2.0 and 1.9%, respectively (Table 3), the spectrum of the Cu-loaded activated carbon is shifted toward lower binding energies, meaning that some of the C−O−P groups of the support are reduced during the copper salt decomposition. For ACCu, the amount of Cu fixed over the activated carbon surface was 1.5 wt % (Table 3). In the case of ACN, a high decrease in the surface P amount is observed (Table 3), along with a positive shift in the P 2p spectrum of ACN (Figure 4A), which is related to the loss of oxidized phosphorus groups via C−O−P bond cleavage during nitro group fixation on the carbon surface, forming a surface phenolic group.[49] To study the copper species present in the ACCu catalyst, a short-exposure XPS analysis was carried out. The Cu 2p XPS spectrum shows the presence of a satellite peak at 9 eV with an area ratio of 0.55 with respect to the main peak, which only appears in Cu^{2+} species. Deconvolution of this spectrum suggests the only presence of this copper oxide (see Figure 4B) because the low temperature of the thermal treatment (450 °C) does not allow the complete reduction of the catalyst in an inert atmosphere.[68] XPS results have also confirmed the successful functionalization of the activated carbon with nitrogen groups, achieving a weight surface concentration of over 2.5% (Table 3). The N 1s region of the XPS spectrum of ACN shows that this nitrogen is mainly introduced as nitro groups (405.7 eV), and less than 15% was found as surface amino groups (399.9 eV) (Figure 4C).[49]

The morphology of the catalysts has been evaluated by TEM (Figure S3B−D). It is observed that the treatment with nitric

https://doi.org/10.1021/acs.energyfuels.4c00108
Energy Fuels 2024, 38, 7018−7032

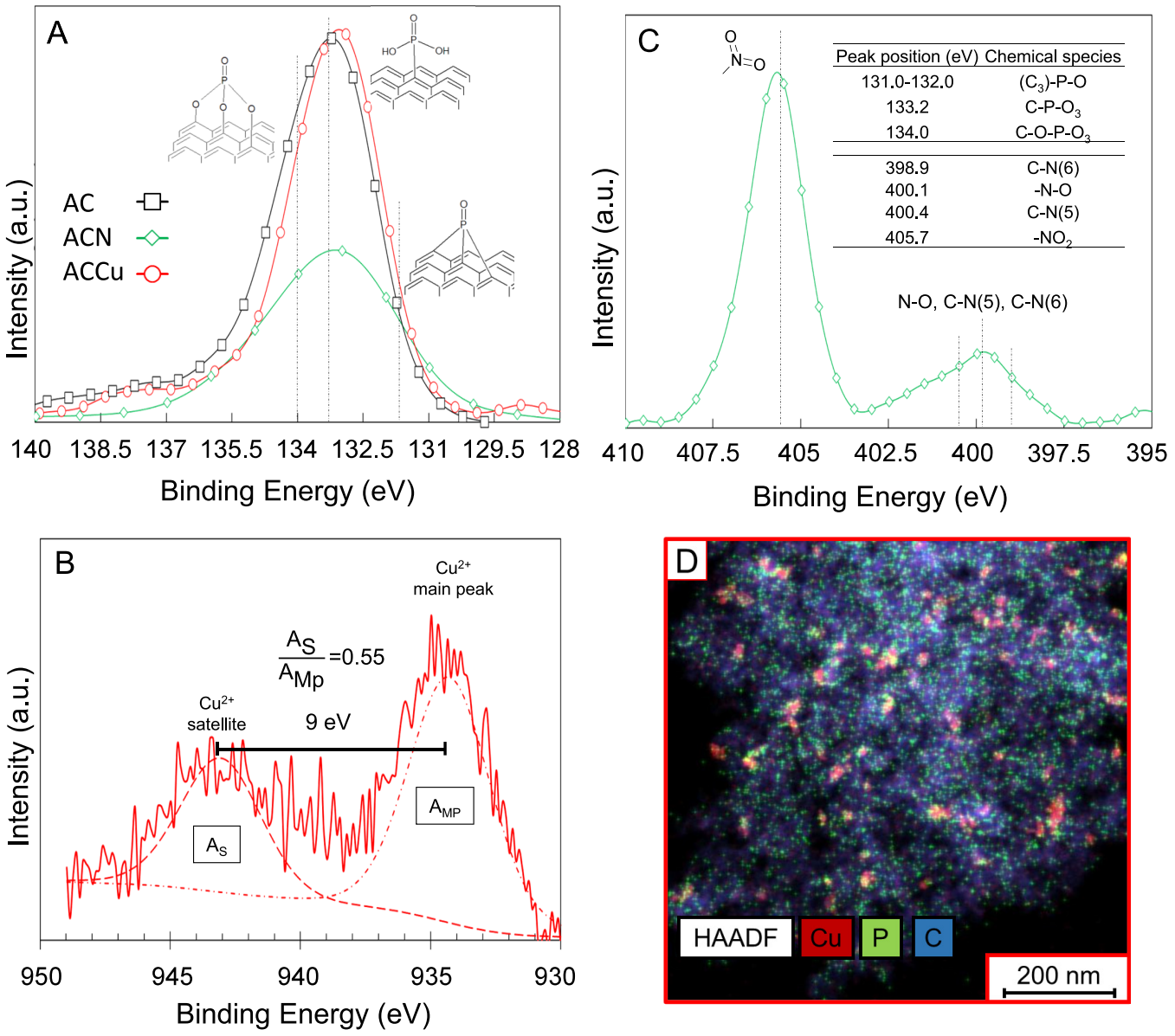

Figure 4. Representative XPS spectra for the P 2p region of AC, ACN, and ACCu (A), for the Cu 2p region of ACCu (B), and for the N 1s region of ACN (C). TEM image with EDX mapping of ACCu (D). Inset in panel (C): summary of the peak position of the different chemical species in P 2p and N 1s regions of the catalysts.

acid does not produce any significant morphology modification compared to the parent activated carbon due to the mild and controlled conditions used for its preparation (Figure S3B,C); in the case of the ACCu catalysts, copper nanoparticles are finely distributed on the catalyst surface, with sizes ranging between 7 and 12 nm (Figure 4D).

Figure 5 represents the CO and CO_2 evolution profiles during the temperature programmed desorption of the carbon materials. In the case of AC, the CO evolution profile presents a main peak at approximately 800 °C corresponding to the thermal reduction of the C−O−P bond of phosphorus surface groups, which confers certain acidity to the activated carbon (Figure 5A).[64,69] Figure 5B shows negligible CO_2 evolution during TPD for AC. Notable changes are observed for ACN. The formation of quinones and phenols due to the elimination of a C−O−P group during the nitration process is denoted by the sharp increase in CO evolution from 600 to 900 °C (Figure 5A). The main change is found in the CO_2-TPD profile (Figure 5B), where a large peak is observed at 300 °C, which has traditionally been related to the decomposition of oxygenated groups such as carboxylic acids, lactone, and anhydrides. The formation of these compounds is widely established in the literature when an activated carbon is treated with nitric acid[70]; however, it was observed that the treatment with HNO_3 to phosphorus-containing activated carbons resulted in the formation of nitro surface groups. The decomposition of these oxygenated surface groups occurs in parallel with the condensation of the nitro ones and the subsequent formation of pyridinic and pyrrole groups.[71] The presence of lactone groups, whose decomposition is associated with the evolution of CO_2 about 400 °C, and anhydride groups, represented by the equimolar evolution of CO and CO_2 at about 550−600 °C, is also observed.[72] In the case of ACCu, the CO evolution peak compared to that observed in the support also increases (Figure 5A), and the total amount of evolved CO is doubled (see Table 3). It is well known in the

https://doi.org/10.1021/acs.energyfuels.4c00108
Energy Fuels 2024, 38, 7018−7032

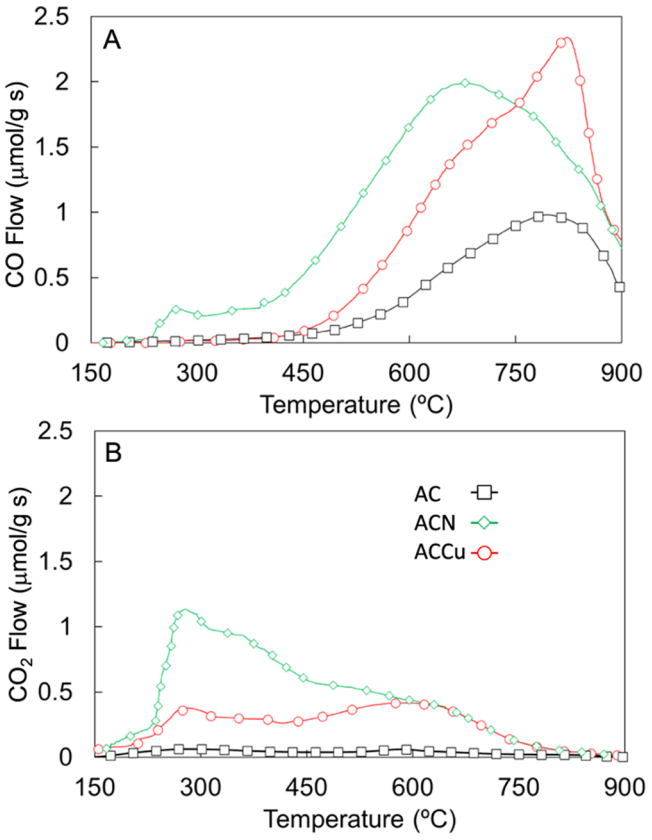

Figure 5. CO (A) and CO_2 (B) evolution as a function of temperature during TPD of AC, ACN, and ACCu.

literature that $Cu(NO_3)_2{\cdot}3H_2O$, used as a precursor of CuO, decomposes above 250 °C, forming CuO.[68] Therefore, the increase in CO evolution can be related to the carbothermic reduction of CuO to Cu_2O (around 550 °C) and to metallic cupper (ca. 650 °C).[68] It is also possible that some phosphorus−copper species can be formed on the surface. In this line, copper phosphate species are known to decompose at temperatures higher than copper oxide,[73] explaining the large CO evolution observed at 780 °C. ACCu also shows a small amount of anhydride groups, as deduced from the small CO_2 peak observed at around 600 °C.

Finally, the catalyst support exhibits moderate acidity and a significant development of the wider porosity; after the copper incorporation, the porosity remains the same, and this copper is mainly Cu^{2+}, which is the active species for lignin oxidative depolymerization reaction. The activated carbon functionalized with nitro groups (ACN) presents wide porosity, similar to its counterpart loaded with copper, showing nitrobenzene-like groups on its surface.

3.3. Oxidative Depolymerization of Lignin. Before the catalytic tests were started, the experimental conditions for the oxidative depolymerization of lignin without solid catalysts were analyzed. To rule out the presence of oxygen mass transfer limitations,[27] three experiments were carried out at 175 °C and 5 bar of initial oxygen pressure under different stirring rates, i.e., 500, 700, and 900 rpm (Figure S4A). Lignin conversion (ca. 40 wt %) and yield to vanillin remained unaltered when the stirring rate was increased from 500 to 900 rpm; consequently, the intermediate speed, 700 rpm, was selected for the rest of the experiments. Temperatures from 125 to 200 °C at a fixed P_{O_2} pressure of 5 bar were tested to evaluate the best operating conditions for maximizing the amount of vanillin in the absence of a heterogeneous catalyst (Figure 6A). The highest amount of vanillin was produced at

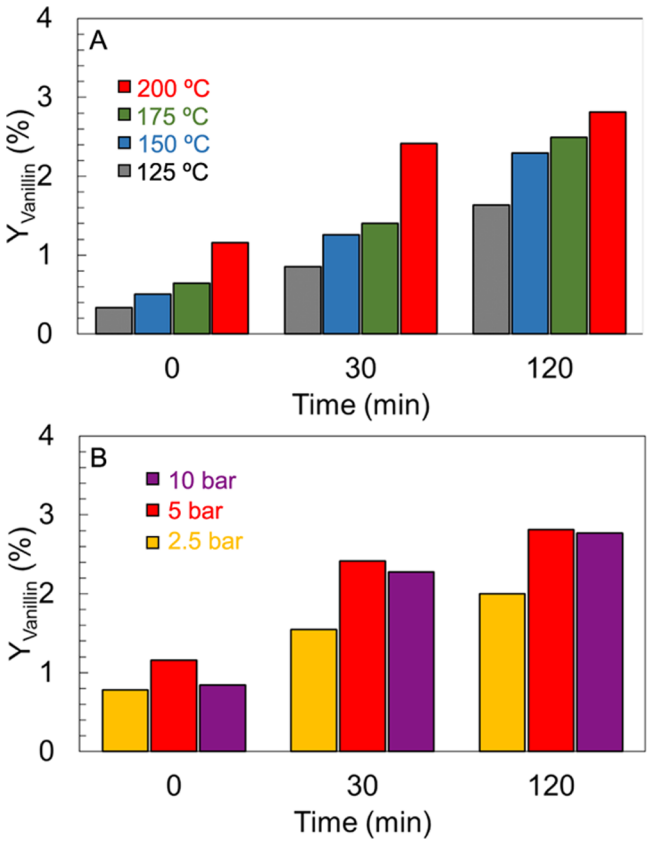

Figure 6. Evolution of the vanillin yield during the oxidative depolymerization of lignin without solid catalysts: at different temperatures (P_{O_2} = 5 bar) (A) and at different initial oxygen pressures with stirring (T = 200 °C) (B).

200 °C. In the case of the oxygen pressure, vanillin yield increases when increasing initial oxygen pressure from 2.5 to 5 bar at 200 °C, with no relevant increase being found at higher pressures (Figure 6B). Under the studied operating conditions, the highest vanillin yield obtained was 2.8%. Note that the use of other lignin feedstocks with larger amounts of β-O-4 and guaiacyl units is needed for achieving higher vanillin yields.[74]

Once the experimental conditions in the absence of a solid catalyst were selected (T = 200 °C and P_{O_2} = 5 bar), oxidative depolymerization reactions were again carried out in the presence of the heterogeneous catalysts. Figure 7A compares the vanillin yield versus reaction time for the process without a solid catalyst, with the catalyst support, and with the copper- and nitro-containing catalysts. As can be seen, the use of AC, which is a carbon chemically activated with a certain acid character,[75] does not produce any increase in lignin conversion (from 41.5 to 41.6% wt), neither improvement in the yield toward vanillin, evidencing that the support does not present catalytic activity. Moreover, even though activated carbons are good adsorbent materials, the lack of changes in vanillin yield with the results in the absence of a solid catalyst suggests that possible adsorption of the reaction products on the carbon materials can be ruled out.

https://doi.org/10.1021/acs.energyfuels.4c00108
Energy Fuels 2024, 38, 7018−7032

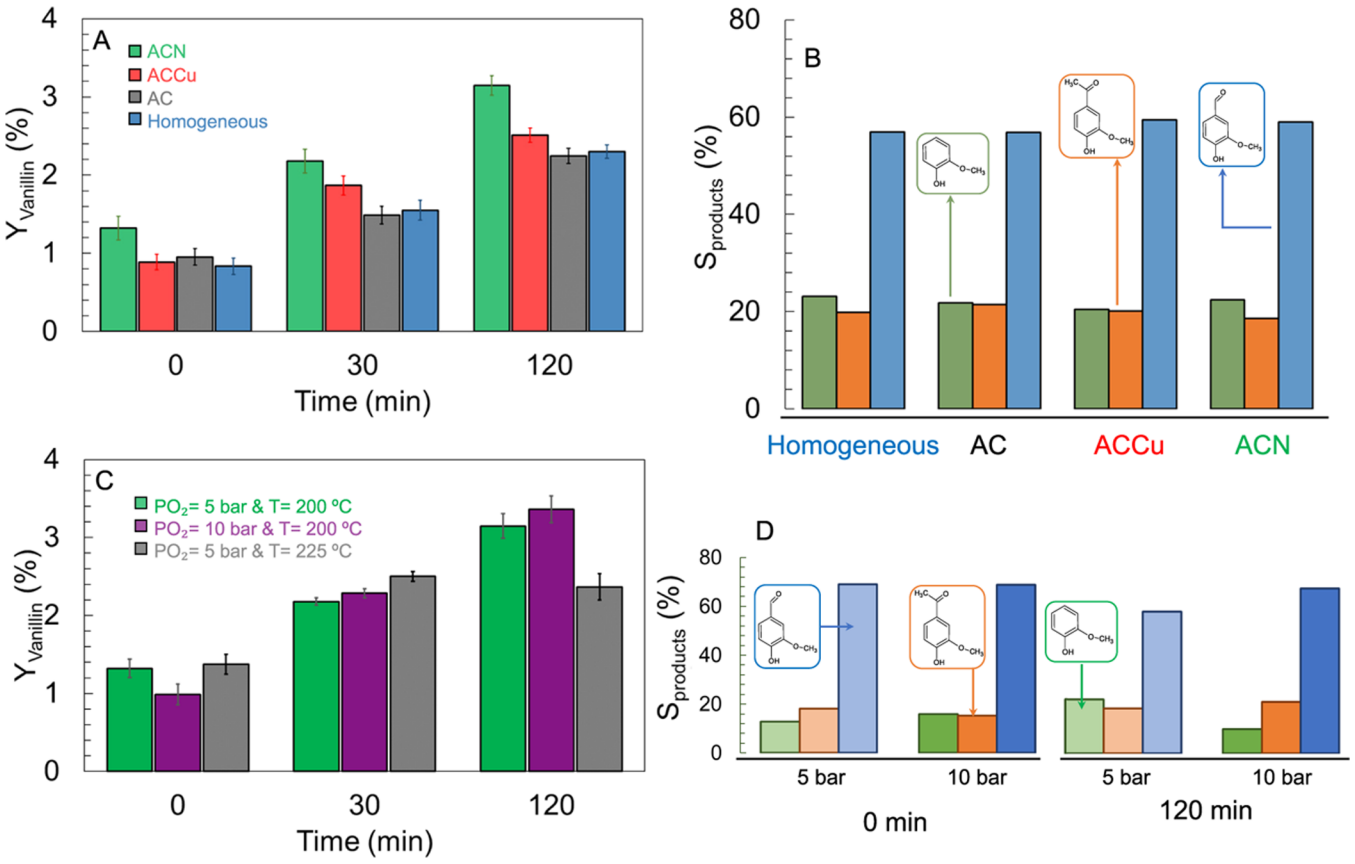

Figure 7. Vanillin yield with and without a heterogeneous catalyst. T = 200 °C and P_{O_2} = 5 bar (A). Vanillin (blue), acetovanillone (orange), and guaiacol (green) selectivity with and without a catalyst at T = 200 °C, P_{O_2} = 5 bar, and a time of reaction of 120 min (B). Vanillin yield during the oxidative depolymerization of lignin. P_{O_2} = 5 bar and T = 200 °C (green), P_{O_2} = 10 bar and T = 200 °C (purple), and P_{O_2} = 5 bar and T = 225 °C (gray) with an ACN catalyst (C). Selectivity toward vanillin (blue), acetovanillone (orange), and guaiacol (green) during the oxidative depolymerization of lignin. T = 200 °C and P_{O_2} = 5 bar and P_{O_2} = 10 bar with an ACN catalyst (D).

As mentioned in Section 1, the catalysts used in this reaction are aimed at increasing selectivity toward vanillin through the oxidation of the phenolate anion, rather than increasing the reaction rate. Thus, the redox potential of the catalyst needs to be high enough for being able to oxidize this anion but as low as possible for avoiding overoxidation of the products. In this sense, the literature points out that supported copper oxide is one of the most effective catalysts owing to the adequate redox potential of the CuO/Cu_2O pair (E^0 = −0.16 eV).[27] When copper is deposited on the catalytic support (ACCu sample), a slight improvement in vanillin production is observed (Figure 7A). However, the nitrogen-doped catalyst (ACN) achieves the highest vanillin production, surpassing the catalyst with copper and reaching yield values as high as 3.2%. The 30% increase in the yield toward vanillin represents a significant improvement regarding those reported in the literature, where the yields toward vanillin with and without a heterogeneous catalyst are hardly ever compared.[76] Nitrogen-doped carbon materials containing quaternary nitrogen groups have been reported to catalyze the biobased vanillin production,[77] but to our knowledge, the oxidative depolymerization of lignin using a modified activated carbon containing nitro groups, prepared in such a simple way and in so few steps, has never been carried out.

Figure 7B represents the selectivity toward the main oxidative depolymerization products in the presence and absence of solid catalysts after 2 h of reaction. Only a slight increase in vanillin selectivity is observed with ACCu, with no variation of the yield toward guaiacol and acetovanillone, suggesting the selective oxidation of phenolate anions to vanillin by copper oxide. In the case of ACN, besides the increase in selectivity toward aldehyde, an increment in selectivity toward guaiacol and acetovanillone is also observed.

To test the behavior of the ACN catalyst under different operating conditions, i.e., initial oxygen pressures and reaction temperature, two new experiments were carried out at a higher initial oxygen pressure of 10 bar, maintaining the same reaction temperature, 200 °C, and increasing the reaction temperature to 225 °C at the same initial oxygen pressures (Figure 7C). When P_{O_2} is increased, the lignin conversion and the yield to vanillin grow significantly at higher pressures, reaching values of 65 and 3.6%, respectively, at 120 min (with a vanillin yield up to 45% higher than that reported without a heterogeneous catalyst). As for the increase in temperature, an initial gain of the yield toward vanillin is observed. However, it decreases at longer reaction times due to the increase in the overoxidation reaction rate,[19] producing a lower vanillin yield than when the reaction proceeded at 200 °C, and the formation of traces of organic acids such as vanillic acid is observed. Figure 7D represents the selectivity toward the main reaction products as a function of the initial oxygen pressure. Selectivity toward vanillin increases with the oxygen pressure. On the other hand, the selectivity to guaiacol is slightly affected by the oxygen

https://doi.org/10.1021/acs.energyfuels.4c00108
Energy Fuels 2024, 38, 7018−7032

pressure; meanwhile, selectivity to acetovanillone does not appear to be significantly different, suggesting the possibility that O_2 is not involved in the reaction pathway of acetovanillone formation.[27]

Direct comparison of the performance of ACN with other catalysts reported in the literature is not straightforward due to the heterogeneity of the technical lignins used as feedstock. A yield to vanillin of 5.2% was obtained with a Pd/CeO_2 catalyst using significantly higher amounts of catalysts (catalyst/organosolv lignin ratio = 2),[76] but they did not compare these results to that obtained without using this catalyst. Another Pd-based catalyst reported a lower yield toward vanillin than without a catalyst.[78] A 3.9% vanillin yield (similar to that presented in this work) was obtained with a steam-explosion lignin using a 5% $CuSO_4/FeCl_3$ (10:1) catalyst.[28] On the other hand, 6.8% vanillin yield was reported using a CuMn(1:3) catalyst,[79] but less than 30% of increment in vanillin yield was achieved when the result is compared to that obtained without a heterogeneous catalyst.

To summarize, it is worth noting that the use of the catalytic support AC in the vanillin production by oxidative depolymerization of lignin did not show an increase in the activity observed in the reaction without a heterogeneous catalyst. This could be related to the activated carbon only presenting some acid groups on its surface (Figure 5), which do not seem to be active in this type of reaction, since it is carried out in an alkaline medium. On the other hand, the ACCu catalyst presents Cu^{2+} (Figure 4B) on its surface, which has been shown to be a great homogeneous and heterogeneous catalyst for this reaction,[80,81] while the ACN catalyst has nitro groups (Figure 4C), similar to nitrobenzene, which is considered to be the most selective chemical agent toward vanillin in oxidative depolymerization of lignin in the literature.[82,83]

3.4. Catalyst Reusability. Once the highest performance of ACN was demonstrated, the reusability of this catalyst was evaluated. With this goal, after a typical run, the catalyst was separated from the liquid phase, i.e., liquid product and solved unreacted lignin, through a filtration process and then washed with distilled water and dried overnight. Afterward, a new reaction under the same previous conditions and 10 bar of oxygen partial pressure was carried out using the used ACN as a catalyst. In this sense, Figure 8A shows the vanillin yield of the oxidative depolymerization of lignin at 10 bar of oxygen partial pressure, 200 °C, and 700 rpm with fresh and used ACN. The used catalyst shows similar catalytic performance, i.e., vanillin yield and products selectivity at 120 min of reaction (see in Figure 8B), to the fresh catalyst, evidencing the possibility of being used in a consecutive cycle without any treatment. The surface chemistry of the catalyst after the reaction was analyzed by XPS (Figure 8C,D). The N 1s XPS region reveals that the nitro group has been completely consumed (405.7 eV) after the end of the first cycle of reaction; meanwhile, the band corresponding to the amine groups has significantly increased (399 eV), which suggests that nitro groups have been fully reduced to amine[71] in an oxygen-free atmosphere. Figure S4B,C shows the pressure inside the reactor, which is the equivalent to the autogenous pressure of the reaction medium (40 g/L NaOH solution) after 60 min of reaction, thus ruling out the presence of oxygen in the gas phase of the reactor and, hence, the one dissolved in the liquid phase. In the case of phosphorus, the shift of the main peak in the P 2p XPS region toward lower binding

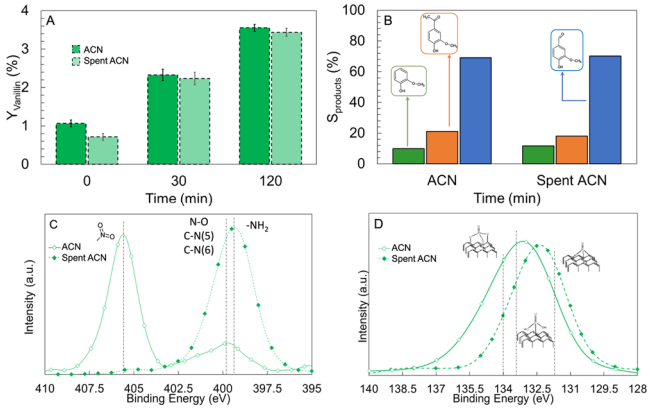

Figure 8. Vanillin yield during the oxidative depolymerization of lignin at 200 °C and 10 bar of oxygen partial pressure with a fresh ACN catalyst and spent ACN (A). Vanillin (blue), acetovanillone (orange), and guaiacol (green) selectivity with fresh and spent ACN catalysts at T = 200 °C, P_{O_2} = 10 bar, and a time of reaction of 120 min (B). Representative XPS spectra for N 1s (C) and P 2p (D) regions of fresh ACN catalyst and used ACN.

energies suggests the formation of more reduced phosphorus species. Since phosphorus groups alone are not active for this reaction (Figure 7) and given the similar activity results after reusing the ACN catalyst, it seems that the active site is formed by the combination of the phosphorus and nitrogen species, which are able to oxidize phenolates to vanillin, producing their own reduction. These reduced species are likely reoxidized in the presence of oxygen during the reaction within a redox cycle. However, if oxygen is totally consumed, then both P and N would remain in a reduced state.

3.5. Proposed Reaction Mechanism. The lignin depolymerization reaction mechanism is useful to understand the different catalytic performance of the tested materials. Lignin depolymerization proceeds in alkaline media through homolytic cleavage, producing monomers, oligomers, and other lignin fragments. Even in the absence of oxidants, some of these monomers can be converted into vanillin. The reaction would begin with the retroaldol cleavage of the α-hydroxy-γ-carbonyl, coming from the homolysis of a β-O-4 bond of the technical lignin structure, which gives rise to a vanillate anion. At the end of the process, as the residual oxidized lignin is precipitated by acidification of the solution, the vanillate anion is protonated, obtaining vanillin. Likewise, acetovanillone production proceeds through the retroaldol cleavage of a α-oxo-β-unsaturated structure, which would explain the suggested nondependence on oxygen partial pressure observed in Figure 7D.[84]

When an oxidant is added to the reaction media, there is an increase in vanillin production due to the oxidation of phenolate anions from the lignin homolysis process, which otherwise would have not directly rendered vanillin. In this mechanism, the oxidant scavenges an electron from the phenolate, promoting the formation of methoxyquinone radicals (Scheme S2). The subsequent nucleophilic addition of the hydroxide ion produces a coniferyl alcohol structure. The oxidation of this alcohol results in the formation of the γ-carbonyl group. This α-unsaturated aldehyde is hydrated, rendering the phenoxyl anion, which in a subsequent step produces the corresponding vanillate anion by retroaldol cleavage. Since this reaction is not catalyzed by acid sites, the role of the carbon support would be merely to provide a high

https://doi.org/10.1021/acs.energyfuels.4c00108
Energy Fuels 2024, 38, 7018−7032

Scheme 1. ACN Catalytic Lignin Depolymerization Reaction Pathway under Excess and Deficiency of Oxygen

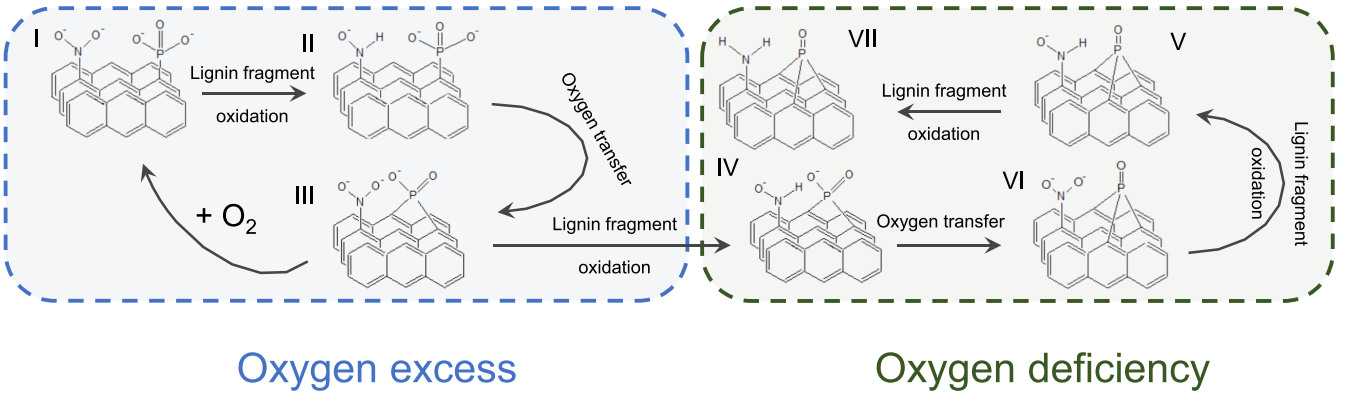

Sample	S	G	Gox	H	β-O-4	β-β	β-5
Kraft L.	0.0	95.9	14.7	4.1	10.6	3.4	2.7
RL	0.0	95.9	43.8	4.1	0.8	1.6	0.0

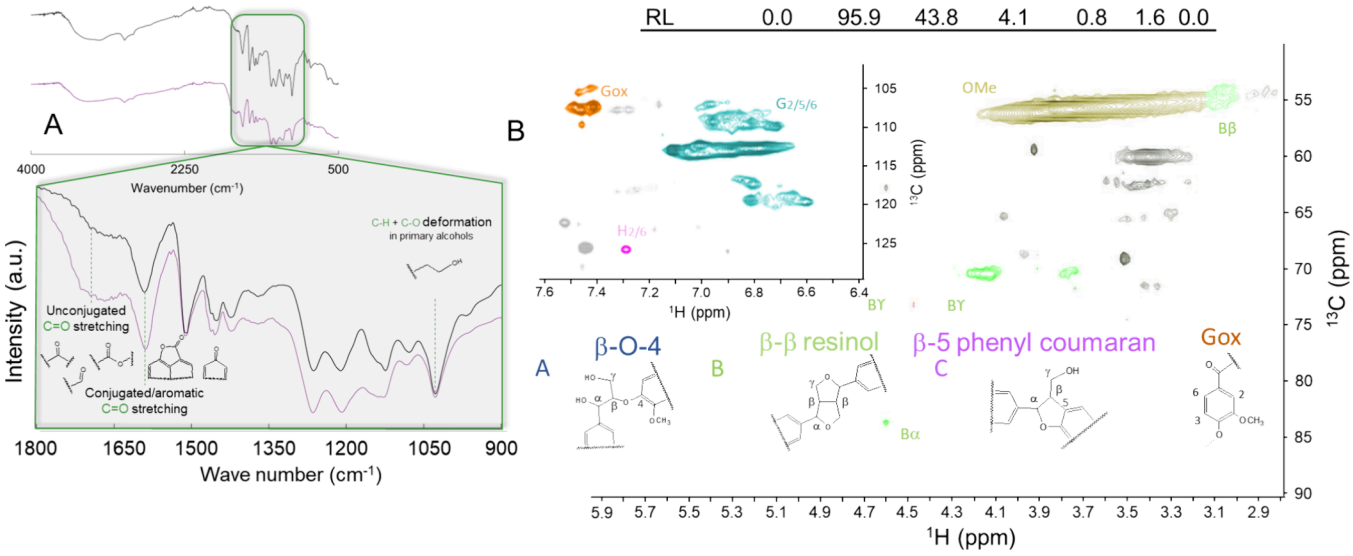

Figure 9. FTIR spectra of Kraft lignin (black line) and reaction residue (purple line) (A). 2D-NMR HSQC spectra of the reaction residue (B). Inset: summary of main units and linkages in Kraft lignin and the reaction residue calculated from NMR HSQC analysis.

dispersion of the active sites (Cu and nitro) and large porosity to avoid diffusional constraints, therefore confirming that only the presence of nitro groups is responsible for the 45% increase in vanillin yield.

The role of the nitro groups during the oxidative depolymerization of lignin could be similar to that of nitrobenzene, which has been used for a long time as an oxidant agent in lignin depolymerization (Scheme S3). The reduction mechanism of nitrobenzene to aniline has been already established in the literature, being summarized in Scheme S3.[85] According to this mechanism, the reduction of the nitro group of the ACN catalyst would end in the formation of an amine group, in agreement with the XPS results of the wasted ACN catalyst in Figure 8C. These amine groups could be reoxidized in the presence of oxygen through the mediation of a phosphorus group (Scheme 1), reactivating the catalyst.

To assess the validity of this hypothesis, two further experiments were carried out with and without an ACN catalyst in the absence of O_2 (Figure S5). The results show that the addition of the catalyst to the reaction media increases the vanillin yield at short times, suggesting that nitro groups are consumed during the production of vanillin. Once active sites are reduced, they cannot be regenerated due to the absence of oxygen in the reaction medium, and no further gain in vanillin yield is obtained. For this reason, it is necessary to consider the reoxidation of amine by oxygen. According to the results obtained, the reaction mechanism summarized in Scheme 1 has been proposed. The reaction mechanism starts with the consumption of one oxygen of the nitro group of species (I), giving rise to species (II). This species is reoxidized by the oxygen of the nearest phosphate group, regenerating the nitro group (III). If oxygen is found in excess in the reaction medium, the phosphorus group is reoxidized with molecular oxygen,[48,69] recovering the species (I). When the oxygen concentration in the reaction medium becomes scarce, the oxidation reaction of the phosphorus group is displaced by the oxidation of a lignin fragment and the consequent reduction of the nitro group, obtaining species (IV). The phosphorus group continues supplying oxygen to the adjoining nitro group until oxygen is depleted, producing species (V), in which phosphorus is in a reduced state, forming C_3P. In the total absence of oxygen in the reaction medium, the nitro group adjacent to C_3P is reduced to an amino species (VII), preceded

https://doi.org/10.1021/acs.energyfuels.4c00108
Energy Fuels 2024, 38, 7018−7032

by the formation of species (VI). Thus, as shown in Figure 8B,C, amino and C_3P groups are detected by XPS due to the depletion of O_2 at the end of the reaction. Finally, the result obtained with the reused catalyst suggests that if oxygen is newly introduced into the reaction medium, species (VII) is able to be reoxidized due to the oxygen capture and transfer capacity of C_3P, being able to produce species (I) again, restarting the catalytic cycle.

3.6. Characterization and Valorization of Residual Lignin. After the reaction, unreacted lignin is isolated and recovered as described in Section 2.1. This residual lignin has been introduced newly into the reaction system, with fresh ACN as a catalyst, and at 200 °C and 10 bar of oxygen partial pressure. At the end of the reaction, the yield to vanillin is negligible (not shown), allowing to conclude that during the first reaction cycle, all the lignin units susceptible to be converted to vanillin had been removed. This residual lignin (RL) has also been characterized to confirm this hypothesis that shows the FTIR spectrum of lignin before and after reaction. Most of the peaks found in the fresh Kraft lignin are maintained, like the peak centered at 1590 cm^{-1}, corresponding to the vibration of the conjugated carbonyl or aromatic group,[58] which seems to have the same intensity before and after oxidation reaction; however, the band associated with the vibration of this group with aliphatic conformations (about 1700 cm^{-1}) becomes wider and more pronounced in lignin after reaction.[58] This change can be associated with the oxidation of side chains under the reaction conditions, which prevails over the oxidation of aromatic units. This last oxidation would favor the rupture of the three-dimensional structure of lignin while maintaining its aromaticity. In addition, the peak centered at 1025 cm^{-1}, corresponding to the linear alcohols,[86] is reduced after the reaction, since it is oxidized, giving rise to a greater amount of linear carbonyl groups. The 2D-NMR HSQC analysis of sample RL shows that despite the moderate yield toward vanillin achieved, the amount of β-O-4 bonds has been considerably reduced (Figure 9B), explaining the negligible production of vanillin when this sample is used again as the reaction feedstock[87] and revealing how the yield achieved toward vanillin cannot be increased with this feedstock.

Based on the physicochemical properties of RL, the possibility of producing an activated carbon under the same conditions as the AC support was studied. Figure 9 reports the comparison of the N_2 adsorption isotherms of AC and activated carbon obtained by chemical activation of the reaction residue (RLC). The N_2 adsorption−desorption isotherms and the derived textural parameters (included as the inset in Figure 10) show well-developed porosity (A_{BET} as high as 1090 m^2/g) and even more developed microporosity than activated carbon from sodium lignosulfonate (V_S = 0.46 cm^3/g). Considering its textural parameters, as well as its rich surface chemistry, with high phosphorus and oxygen surface contents measured by XPS (3.4 and 13.2% of mass surface concentration of P and O, respectively, see Figure S6), the obtained AC has potential applications such as adsorption of pollutants in gaseous or liquid effluents or as catalytic support. In this way, the residue from the production of biobased vanillin would be used, contributing to the circular economy and to a zero-waste process.

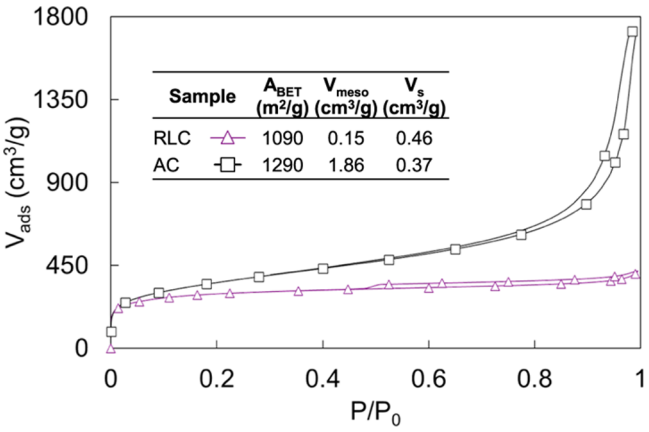

Figure 10. N_2 adsorption−desorption isotherms obtained at −196 °C of RLC and AC. Inset: main textural parameters of RLC and AC.

4. CONCLUSIONS

The production of biobased vanillin from the oxidative depolymerization of Kraft lignin was studied in a batch reactor. For this purpose, an activated carbon obtained by chemical activation of a sodium lignosulfonate with phosphoric acid (A_{BET}= 1290 m^2/g and V_{meso} = 1.86 cm^3/g) was used as support of two different types of catalysts. The first catalyst consists of a functionalization with nitric acid of the phosphorus containing activated carbon, resulting into nitrobenzene-like structures bonded to the carbon surface (2.5 and 1.25% of surface nitrogen and phosphorus respectively, measured by XPS). This functionalization allows the heterogenization of nitrobenzene structures on the activated carbon, avoiding the use of alkaline nitrobenzene oxidation, which can produce strong environmental impacts. The second one is a copper catalyst with 5 wt %, mainly as copper oxide.

A vanillin yield at least 30% higher than that obtained in the homogeneous (noncatalyzed) reaction was obtained with the catalyst functionalized with nitro groups (ACN), with this amount being the maximum yield obtainable with this technical lignin (3.6%). Although this type of lignin is not the most adequate to produce vanillin, in the context of a lignocellulosic biorefinery, the largest market of it could make its use a very profitable option.

The behavior of ACN was tested in subsequent runs under the same reaction conditions without any regeneration treatment, maintaining the same activity (deviation error lower than 5%). The postreaction XPS analysis and the catalytic results suggested that the nitro groups present on the catalyst were responsible for the catalyzed formation of vanillin, while phosphorus groups present on the activated carbon acted as an oxygen mediator for the regeneration of the nitro group.

Within the framework of green chemistry and zero waste processes, residual lignin (RL) was also used as feedstock in the production of a new activated carbon. This AC showed a high specific surface area (A_{BET} = 1090 m^2/g) and rich surface chemistry (P = 3.4% and O = 13.2% measured by XPS), making it a promising material for liquid- or gas-phase pollutant removal by adsorption and/or catalysis.

https://doi.org/10.1021/acs.energyfuels.4c00108
Energy Fuels 2024, 38, 7018−7032

■ ASSOCIATED CONTENT

Supporting Information

The Supporting Information is available free of charge at https://pubs.acs.org/doi/10.1021/acs.energyfuels.4c00108.

Detailed experimental procedures; reaction mechanisms for oxidative depolymerization of lignin; GC-MS chromatograms; TEM images; XPS spectra; DTP-NH_3 and chemical reaction data (PDF)

■ AUTHOR INFORMATION

Corresponding Author

Juana M. Rosas − *Departamento de Ingeniería Química, Campus de Teatinos s/n, Universidad de Málaga, Andalucía Tech., Málaga 29010, Spain;* orcid.org/0000-0001-9158-3413; Email: jmrosas@uma.es

Authors

Miguel García-Rollán − *Departamento de Ingeniería Química, Campus de Teatinos s/n, Universidad de Málaga, Andalucía Tech., Málaga 29010, Spain*

Maria N. Rivas-Márquez − *Departamento de Ingeniería Química, Campus de Teatinos s/n, Universidad de Málaga, Andalucía Tech., Málaga 29010, Spain*

Salvador Bertran-Llorens − *Department of Chemical Engineering, ENTEG, University of Groningen, Groningen 9747 AG, Netherlands;* orcid.org/0000-0001-6514-7976

Peter J. Deuss − *Department of Chemical Engineering, ENTEG, University of Groningen, Groningen 9747 AG, Netherlands;* orcid.org/0000-0002-2254-2500

Ramiro Ruiz-Rosas − *Departamento de Ingeniería Química, Campus de Teatinos s/n, Universidad de Málaga, Andalucía Tech., Málaga 29010, Spain;* orcid.org/0000-0001-8433-1808

José Rodríguez-Mirasol − *Departamento de Ingeniería Química, Campus de Teatinos s/n, Universidad de Málaga, Andalucía Tech., Málaga 29010, Spain;* orcid.org/0000-0003-3122-1220

Tomás Cordero − *Departamento de Ingeniería Química, Campus de Teatinos s/n, Universidad de Málaga, Andalucía Tech., Málaga 29010, Spain;* orcid.org/0000-0002-3557-881X

Complete contact information is available at: https://pubs.acs.org/10.1021/acs.energyfuels.4c00108

Author Contributions

M.G.-R.: investigation, methodology, and writing of the original draft. N.R.-M.: investigation and methodology. S.B.-L.: investigation. P.J.D.: review, editing, and supervision. R.R.-R.: formal analysis, validation, and supervision. J.M.R.: conceptualization, review and editing, and supervision. J.R.-M.: review, editing, and supervision. T.C.: conceptualization, resources, and project administration.

Notes

The authors declare no competing financial interest.

■ ACKNOWLEDGMENTS

The authors wish to thank MICINN (RTI2018-097555-B-100) and Junta de Andalucía (UMA18-FEDERJA-110 and P18-RT-4592) for financial support. Funding for open access charge: Universidad de Málaga/CBUA. M.G.-R. acknowledges the assistance of MICINN through an FPU Grant (FPU 18/01402).

■ REFERENCES

(1) dos SantosAbreu, H.; Do Nascimento, A. M.; Maria, M. A. Lignin structure and wood properties. *Wood Fiber Sci.* **1999**, *31*, 426−433.

(2) Higuchi, T. Lignin biochemistry: biosynthesis and biodegradation. *Wood Science and Technology* **1990**, *24*, 23−63.

(3) Chakar, F. S.; Ragauskas, A. J. Review of current and future softwood kraft lignin process chemistry. *Industrial Crops and Products* **2004**, *20*, 131−141.

(4) Adler, E. Lignin chemistry—past, present and future. *Wood Science and Technology* **1977**, *11*, 169−218.

(5) Lapierre, C.; Application of new methods for the investigation of lignin structure. *Forage Cell Wall Structure and Digestibility*; 1993. pp. 133-166 DOI: 10.2134/1993.foragecellwall.c6

(6) Heeres, A.; Schenk, N.; Muizebelt, I.; Blees, R.; De Waele, B.; Zeeuw, A. J.; Meyer, N.; Carr, R.; Wilbers, E.; Heeres, H. J. Synthesis of bio-aromatics from black liquors using catalytic pyrolysis. *ACS Sustainable Chem. Eng.* **2018**, *6*, 3472−3480.

(7) Furusawa, T.; Sato, T.; Sugito, H.; Miura, Y.; Ishiyama, Y.; Sato, M.; Itoh, N.; Suzuki, N. Hydrogen production from the gasification of lignin with nickel catalysts in supercritical water. *Int. J. Hydrogen Energy* **2007**, *32*, 699−704.

(8) Chowdari, R. K.; Agarwal, S.; Heeres, H. J. Hydrotreatment of kraft lignin to alkylphenolics and aromatics using Ni, Mo, and W phosphides supported on activated carbon. *ACS Sustainable Chem. Eng.* **2019**, *7*, 2044−2055.

(9) Figueirêdo, M. B.; Jotic, Z.; Deuss, P. J.; Venderbosch, R. H.; Heeres, H. J. Hydrotreatment of pyrolytic lignins to aromatics and phenolics using heterogeneous catalysts. *Fuel Process. Technol.* **2019**, *189*, 28−38.

(10) Xu, X.; Li, P.; Zhong, Y.; Yu, J.; Miao, C.; Tong, G. Review on the oxidative catalysis methods of converting lignin into vanillin. *Int. J. Biol. Macromol.* **2023**, *243*, No. 125203.

(11) Fache, M.; Boutevin, B.; Caillol, S. Vanillin production from lignin and its use as a renewable chemical. *ACS Sustainable Chem. Eng.* **2016**, *4*, 35−46.

(12) Borges da Silva, E. A.; Zabkova, M.; Araújo, J. D.; Cateto, C. A.; Barreiro, M. F.; Belgacem, M. N.; Rodrigues, A. E. An integrated process to produce vanillin and lignin-based polyurethanes from kraft lignin. *Chem. Eng. Res. Des.* **2009**, *87*, 1276−1292.

(13) Fache, M.; Darroman, E.; Besse, V.; Auvergne, R.; Caillol, S.; Boutevin, B. Vanillin, a promising biobased building-block for monomer synthesis. *Green Chem.* **2014**, *16*, 1987−1998.

(14) Mialon, L.; Pemba, A. G.; Miller, S. A. Biorenewable polyethylene terephthalate mimics derived from lignin and acetic acid. *Green Chem.* **2010**, *12*, 1704−1706.

(15) Rodrigues, A. E.; Pinto, P.; Barreiro, M. F.; Esteves da Costa, C. A.; Ferreira da Mota, M. I.; Fernandes, I. *An integrated approach for added-value products from lignocellulosic biorefineries*. Springer Cham; 2018. DOI: 10.1007/978-3-319-99313-3.

(16) Mehta, M. J.; Kulshrestha, A.; Sharma, S.; Kumar, A. Room temperature depolymerization of lignin using a protic and metal based ionic liquid system: an efficient method of catalytic conversion and value addition. *Green Chem.* **2021**, *23*, 1240−1247.

(17) Pinto, P. C. R.; Costa, C. E.; Rodrigues, A. E. Oxidation of lignin from eucalyptus globulus pulping liquors to produce syringaldehyde and vanillin. *Ind. Eng. Chem. Res.* **2013**, *52*, 4421−4428.

(18) Bjørsvik, H.-R.; Minisci, F. Fine chemicals from lignosulfonates. 1. Synthesis of vanillin by oxidation of lignosulfonates. *Org. Proc. Res. Dev.* **1999**, *3*, 330−340.

(19) Fargues, C.; Mathias, Á.; Silva, J.; Rodrigues, A. Kinetics of vanillin oxidation. *Chem. Eng. Technol.* **1996**, *19*, 127−36.

(20) Pepper, J. M.; Casselman, B. W.; Karapally, J. C. Lignin oxidation. Preferential use of cupric oxide. *Can. J. Chem.* **1967**, *45*, 3009−3012.

(21) Zhang, R.; Maltari, R.; Guo, M.; Kontro, J.; Eronen, A.; Repo, T. Facile synthesis of vanillin from fractionated Kraft lignin. *Industrial Crops and Products* **2020**, *145*, No. 112095.

(22) Zirbes, M.; Graßl, T.; Neuber, R.; Waldvogel, S. R. Peroxodicarbonate as a Green Oxidizer for the Selective Degradation of Kraft Lignin into Vanillin. *Angew. Chem., Int. Ed.* **2023**, *62*, No. e202219217.
(23) Leopold, B. Studies on lignin. iii. Oxidation of wood from Picea abies (L.) Karst. (Norway Spruce) with nitribenzene and alkali. *Acta Chem. Scand.* **1952**, *6*, 38−48.
(24) Tarabanko, V. E.; Koropatchinskaya, N. V.; Kudryashev, A. V.; Kuznetsov, B. N. Influence of lignin origin on the efficiency of the catalytic oxidation of lignin into vanillin and syringaldehyde. *Russ. Chem. Bull.* **1995**, *44*, 367−371.
(25) Yamamoto, K.; Hosoya, T.; Yoshioka, K.; Miyafuji, H.; Ohno, H.; Yamada, T. Tetrabutylammonium hydroxide 30-hydrate as novel reaction medium for lignin conversion. *ACS Sustainable Chem. Eng.* **2017**, *5*, 10111−10115.
(26) Mathieu, Y.; Vidal, J. D.; Arribas Martínez, L.; Abad Fernández, N.; Iborra, S.; Corma, A. Molecular oxygen lignin depolymerization: an insight into the stability of phenolic monomers. *ChemSusChem* **2020**, *13*, 4743−4758.
(27) Tarabanko, V. E.; Tarabanko, N. Catalytic oxidation of lignins into the aromatic aldehydes: General process trends and development prospects. *International Journal of Molecular Sciences* **2017**, *18*, 2421.
(28) Wu, G.; Heitz, M.; Chornet, E. Improved alkaline oxidation process for the production of aldehydes (vanillin and syringaldehyde) from steam-explosion hardwood lignin. *Ind. Eng. Chem. Res.* **1994**, *33*, 718−723.
(29) Zhao, Y.; Xu, Q.; Pan, T.; Zuo, Y.; Fu, Y.; Guo, Q. X. Depolymerization of lignin by catalytic oxidation with aqueous polyoxometalates. *Applied Catalysis A: General* **2013**, *467*, 504−508.
(30) Voitl, T.; von Rohr, P. R. Demonstration of a process for the conversion of kraft lignin into vanillin and methyl vanillate by acidic oxidation in aqueous methanol. *Ind. Eng. Chem. Res.* **2010**, *49*, 520−525.
(31) Zhang, Z.; Gogoi, P.; Geng, Z.; Liu, X.; Du, X. Low temperature lignin depolymerization to aromatic compounds with a redox couple catalyst. *Fuel* **2020**, *281*, No. 118799.
(32) Tang, B.; Li, W.; Zhang, X.; Zhang, B.; Zhang, H.; Li, C. Depolymerization of Kraft lignin to liquid fuels with MoS_2 derived oxygen-vacancy-enriched MoO_3 in a hydrogen-donor solvent system. *Fuel* **2022**, *324*, No. 124674.
(33) Rawat, S.; Gupta, P.; Singh, B.; Bhaskar, T.; Natte, K.; Narani, A. Molybdenum-catalyzed oxidative depolymerization of alkali lignin: Selective production of Vanillin. *Applied Catalysis A: General* **2020**, *598*, No. 117567.
(34) Bhargava, S.; Jani, H.; Tardio, J.; Akolekar, D.; Hoang, M. Catalytic wet oxidation of ferulic acid (a model lignin compound) using heterogeneous copper catalysts. *Ind. Eng. Chem. Res.* **2007**, *46*, 8652−8656.
(35) Wang, N.; Xue, R.; Yang, N.; Sun, H.; Zhang, B.; Ma, Z.; Ma, Y.; Zang, L. Efficient oxidative cleavage of lignin C-C model compound using MOF-derived Cobalt/Nickel sulfide heterostructures. *J. Alloys Compd.* **2022**, *929*, No. 167324.
(36) Zhou, M.; Tang, C.; Xia, H.; Li, J.; Liu, J.; Jiang, J.; Zhao, J.; Yang, X.; Chen, C. Ni-based MOFs catalytic oxidative cleavage of lignin models and lignosulfonate under oxygen atmosphere. *Fuel* **2022**, *320*, No. 123993.
(37) Zhang, Y.; Yue, H.; Zou, J.; Yao, R.; Duan, W.; Ma, H.; Zhao, Y.; He, Z. Oxidative lignin depolymerization using metal supported hydrotalcite catalysts: Effects of process parameters on phenolic compounds distribution. *Fuel* **2023**, *331*, No. 125805.
(38) Luo, J.; Melissa, P.; Zhao, W.; Wang, Z.; Zhu, Y. Selective lignin oxidation towards vanillin in phenol media. *ChemistrySelect* **2016**, *1*, 4596−4601.
(39) Suhas; Carrott, P. J. M.; Ribeiro Carrott, M. M. L. Lignin − from natural adsorbent to activated carbon: a review. *Bioresour. Technol.* **2007**, *98*, 2301−2312.
(40) Rodríguez, J. J.; Cordero, T.; Rodríguez-Mirasol, José Carbon materials from lignin and their applications. *Prod. Biofuels Chem. Lignin* **2016**, *6*, 217.
(41) Gonzalez-Serrano, E.; Cordero, T.; Rodriguez-Mirasol, J.; Cotoruelo, L.; Rodriguez, J. J. Removal of water pollutants with activated carbons prepared from H_3PO_4 activation of lignin from kraft black liquors. *Water Res.* **2004**, *38*, 3043−3050.
(42) Salinas-Torres, D.; Ruiz-Rosas, R.; Valero-Romero, M. J.; Rodríguez-Mirasol, J.; Cordero, T.; Morallón, E.; Cazorla-Amorós, D. Asymmetric capacitors using lignin-based hierarchical porous carbons. *J. Power Sources* **2016**, *326*, 641−651.
(43) Torres-Liñán, J.; García-Rollán, M.; Rosas, J. M.; Rodríguez-Mirasol, J.; Cordero, T. Deactivation of a biomass-derived zirconium-doped phosphorus-containing carbon catalyst in the production of dimethyl ether from methanol dehydration. *Energy Fuels* **2021**, *35*, 17225−17240.
(44) Bedia, J.; Ruiz-Rosas, R.; Rodríguez-Mirasol, J.; Cordero, T. Kinetic study of the decomposition of 2-butanol on carbon-based acid catalyst. *AIChE J.* **2010**, *56*, 1557−1568.
(45) Cao, Y.; Chen, S. S.; Tsang, D. C. W.; Clark, J. H.; Budarin, V. L.; Hu, C.; Wu, K. C. W.; Zhang, S. Microwave-assisted depolymerization of various types of waste lignins over two-dimensional CuO/BCN catalysts. *Green Chem.* **2020**, *22*, 725−736.
(46) Sun, K.; Chen, S.; Zhang, J.; Lu, G. P.; Cai, C. Cobalt nanoparticles embedded in N-doped porous carbon derived from bimetallic zeolitic imidazolate frameworks for one-pot selective oxidative depolymerization of lignin. *ChemCatChem.* **2019**, *11*, 1264−1271.
(47) Zeng, J.; Tong, Z.; Bao, H.; Chen, N.; Wang, F.; Wang, Y.; Xiao, D. Controllable depolymerization of lignin using carbocatalyst graphene oxide under mild conditions. *Fuel* **2020**, *267*, No. 117100.
(48) Rosas, J. M.; Ruiz-Rosas, R.; Rodríguez-Mirasol, J.; Cordero, T. Kinetic study of the oxidation resistance of phosphorus-containing activated carbons. *Carbon* **2012**, *50*, 1523−1537.
(49) Ternero-Hidalgo, J. J.; Rosas, J. M.; Palomo, J.; Valero-Romero, M. J.; Rodríguez-Mirasol, J.; Cordero, T. Functionalization of activated carbons by HNO_3 treatment: Influence of phosphorus surface groups. *Carbon* **2016**, *101*, 409−419.
(50) Jagiello, J.; Ania, C.; Parra, J. B.; Cook, C. Dual gas analysis of microporous carbons using 2D-NLDFT heterogeneous surface model and combined adsorption data of N_2 and CO_2. *Carbon* **2015**, *91*, 330−337.
(51) Tofani, G.; Jasiukaitytė-Grojzdek, E.; Grilc, M.; Likozar, B. Organosolv biorefinery: resource-based process optimization, pilot technology scale-up and economics. *Green Chem.* **2024**, *26*, 186−201.
(52) Zijlstra, D. S.; Lahive, C. W.; Analbers, C. A.; Figueirêdo, M. B.; Wang, Z.; Lancefield, C. S.; Deuss, P. J. Mild Organosolv lignin extraction with alcohols: the importance of benzylic alkoxylation. *ACS Sustainable Chem. Eng.* **2020**, *8*, 5119−5131.
(53) Lancefield, C. S.; Panovic, I.; Deuss, P. J.; Barta, K.; Westwood, N. J. Pre-treatment of lignocellulosic feedstocks using biorenewable alcohols: towards complete biomass valorisation. *Green Chem.* **2017**, *19*, 202−214.
(54) Rodríguez-Mirasol, J.; Cordero, T.; Rodríguez, J. J. Preparation and characterization of activated carbons from eucalyptus kraft lignin. *Carbon* **1993**, *31*, 87−95.
(55) Zhang, H.; Bai, Y.; Zhou, W.; Chen, F. Color reduction of sulfonated eucalyptus kraft lignin. *Int. J. Biol. Macromol.* **2017**, *97*, 201−208.
(56) NYQUIST, R.; Nyquist, R. A. Thiols, sulfides and disulfides, alkanethiols, and alkanedithiols (S-H stretching). *Interpreting infrared, raman, and nuclear magnetic resonance spectra*. Academic Press **2001**:2, 65−83. DOI: 10.1016/B978-012523475-7/50184-4.
(57) Pandey, K. K. A study of chemical structure of soft and hardwood and wood polymers by FTIR Spectroscopy. *J. Appl. Polym. Sci.* **1969**, *71*, 1969−1975.
(58) Monteil-Rivera, F.; Phuong, M.; Ye, M.; Halasz, A.; Hawari, J. Isolation and characterization of herbaceous lignins for applications in biomaterials. *Industrial Crops and Products* **2013**, *41*, 356−364.
(59) Wang, Z.; Zhu, X.; Deuss, P. J. The effect of ball milling on birch, pine, reed, walnut shell enzymatic hydrolysis recalcitrance and

https://doi.org/10.1021/acs.energyfuels.4c00108
Energy Fuels 2024, 38, 7018−7032

the structure of the isolated residual enzyme lignin. *Industrial Crops and Products* **2021**, *167*, No. 113493.
(60) Thommes, M.; Kaneko, K.; Neimark, A. V.; Olivier, J. P.; Rodriguez-Reinoso, F.; Rouquerol, J.; Sing, K. S. W. Physisorption of gases, with special reference to the evaluation of surface area and pore size distribution (IUPAC Technical Report). *Pure Appl. Chem.* **2015**, *87*, 1051−1069.
(61) Hernández Mañas, A.; Vilcocq, L.; Fongarland, P.; Djakovitch, L. Lignin catalytic oxidation by CuO/TiO_2: role of catalyst in phenolics formation. *Waste Biomass Valorization* **2023**, *14*, 3789−3809.
(62) Cazorla-Amorós, D.; Alcañiz-Monge, J.; de La Casa-Lillo, M. A.; Linares-Solano, A. CO_2 As an adsorptive to characterize carbon molecular sieves and activated carbons. *Langmuir* **1998**, *14*, 4589−4596.
(63) Puziy, A. M.; Poddubnaya, O. I.; Ziatdinov, A. M. On the chemical structure of phosphorus compounds in phosphoric acid-activated carbon. *Appl. Surf. Sci.* **2006**, *252*, 8036−8038.
(64) Bedia, J.; Rosas, J. M.; Márquez, J.; Rodríguez-Mirasol, J.; Cordero, T. Preparation and characterization of carbon based acid catalysts for the dehydration of 2-propanol. *Carbon* **2009**, *47*, 286−294.
(65) Puziy, A. M.; Poddubnaya, O. I.; Martínez-Alonso, A.; Suárez-García, F.; Tascón, J. M. D. Surface chemistry of phosphorus-containing carbons of lignocellulosic origin. *Carbon* **2005**, *43*, 2857−2868.
(66) Wu, X.; Radovic, L. R. Inhibition of catalytic oxidation of carbon/carbon composites by phosphorus. *Carbon* **2006**, *44*, 141−151.
(67) Bedia, J.; Rosas, J. M.; Vera, D.; Rodríguez-Mirasol, J.; Cordero, T. Isopropanol decomposition on carbon based acid and basic catalysts. *Catal. Today* **2010**, *158*, 89−96.
(68) Morozov, I. V.; Znamenkov, K. O.; Korenev, Y. M.; Shlyakhtin, O. A. Thermal decomposition of Cu(NO3)2·3H2O at reduced pressures. *Thermochim. Acta* **2003**, *403*, 173−179.
(69) Valero-Romero, M. J.; García-Mateos, F. J.; Rodríguez-Mirasol, J.; Cordero, T. Role of surface phosphorus complexes on the oxidation of porous carbons. *Fuel Process. Technol.* **2017**, *157*, 116−126.
(70) Moreno-Castilla, C.; López-Ramón, M. V.; Carrasco-Marín, F. Changes in surface chemistry of activated carbons by wet oxidation. *Carbon* **2000**, *38*, 1995−2001.
(71) Palomo, J.; Ternero-Hidalgo, J. J.; Rosas, J. M.; Rodríguez-Mirasol, J.; Cordero, T. Selective nitrogen functionalization of phosphorus-containing activated carbons. *Fuel Process. Technol.* **2017**, *156*, 438−445.
(72) Figueiredo, J. L.; Pereira, M. F. R.; Freitas, M. M. A.; Orfao, J. J. M. Modification of the surface chemistry of activated carbons. *Carbon* **1999**, *37*, 1379−1389.
(73) Bamberger, C. E.; Specht, E. D.; Anovitz, L. M. Crystalline copper phosphates: synthesis and thermal stability. *J. Am. Ceram. Soc.* **1997**, *80*, 3133−3138.
(74) Rodrigues-Pinto, P. C.; Borges Da Silva, E. A.; Rodrigues, A. E. Insights into oxidative conversion of lignin to high-added-value phenolic aldehydes. *Ind. Eng. Chem. Res.* **2011**, *50*, 741−748.
(75) Bedia, J.; Barrionuevo, R.; Rodríguez-Mirasol, J.; Cordero, T. Ethanol dehydration to ethylene on acid carbon catalysts. *Applied Catalysis B: Enviromental* **2011**, *103*, 302−310.
(76) Deng, W.; Zhang, H.; Wu, X.; Li, R.; Zhang, Q.; Wang, Y. Oxidative conversion of lignin and lignin model compounds catalyzed by CeO_2-supported Pd nanoparticles. *Green Chem.* **2015**, *17*, 5009−5018.
(77) Gao, Y.; Zhang, J.; Chen, X.; Ma, D.; Yan, N. A Metal-Free, Carbon-based catalytic system for the oxidation of lignin model compounds and lignin. *ChemPlusChem.* **2014**, *79*, 825−834.
(78) Bourbiaux, D.; Xu, Y.; Burel, L.; Goc, F.; Fongarland, P.; Philippe, R.; Aubert, G.; Aymonier, C.; Rataboul, F.; Djakovitch, L. Investigating (Pseudo)-heterogeneous pd-catalysts for kraft lignin depolymerization under mild aqueous basic conditions. *Catalysts* **2021**, *11*, 1311.
(79) Jeon, W.; Choi, I. H.; Park, J. Y.; Lee, J. S.; Hwang, K. R. Alkaline wet oxidation of lignin over Cu-Mn mixed oxide catalysts for production of vanillin. *Catal. Today* **2020**, *352*, 95−103.
(80) Tarabanko, V. E.; Kaygorodov, K. L.; Kazachenko, A. S.; Smirnova, M. A.; Chelbina, Y. V.; Kosivtsov, Y.; Golubkov, V. A. Mass transfer in the processes of native lignin oxidation into vanillin via oxygen. *Catalysts* **2023**, *13*, 1490.
(81) Walch, F.; Abdelaziz, O. Y.; Meier, S.; Bjelić, S.; Hulteberg, C. P.; Riisager, A. Oxidative depolymerization of Kraft lignin to high-value aromatics using a homogeneous vanadium−copper catalyst. *Catalysis Science and Technology* **2021**, *11*, 1843−1853.
(82) Costa, C. A. E.; Casimiro, F. M.; Vega-Aguilar, C.; Rodrigues, A. E. Lignin valorization for added-value chemicals: Kraft lignin versus lignin fractions. *ChemEngineering* **2023**, *7*, 42.
(83) Hayashi, T.; Hosoya, T.; Miyafuji, H. Vanillin production pathways in alkaline nitrobenzene oxidation of guaiacylglycerol-β-guaiacyl ether. *J. Agric. Food Chem.* **2023**, *71*, 10124−10132.
(84) More, A.; Elder, T.; Jiang, Z. Towards a new understanding of the retro-aldol reaction for oxidative conversion of lignin to aromatic aldehydes and acids. *Int. J. Biol. Macromol.* **2021**, *183*, 1505−1513.
(85) Schultz, T. P.; Templeton, M. C. Proposed mechanism for the nitrobenzene oxidation of lignin. *Holzforschung* **1986**, *40*, 93−97.
(86) Chua, Y. W.; Yu, Y.; Wu, H. Thermal decomposition of pyrolytic lignin under inert conditions at low temperatures. *Fuel* **2017**, *200*, 70−75.
(87) Wang, Y.; Sun, S.; Li, F.; Cao, X.; Sun, R. Production of vanillin from lignin: The relationship between β-O-4 linkages and vanillin yield. *Industrial Crops and Products* **2018**, *116*, 116−121.

https://doi.org/10.1021/acs.energyfuels.4c00108
Energy Fuels 2024, 38, 7018−7032